

Caractérisation de dépôts et poussières produites par les plasmas de tokamak

Andrea Campos





Cécile Arnas, Céline Martin



Mathilde Diez, Bernard Pegourié,
Elodie Bernard, Emmanuelle Tsitrone,
the WEST team



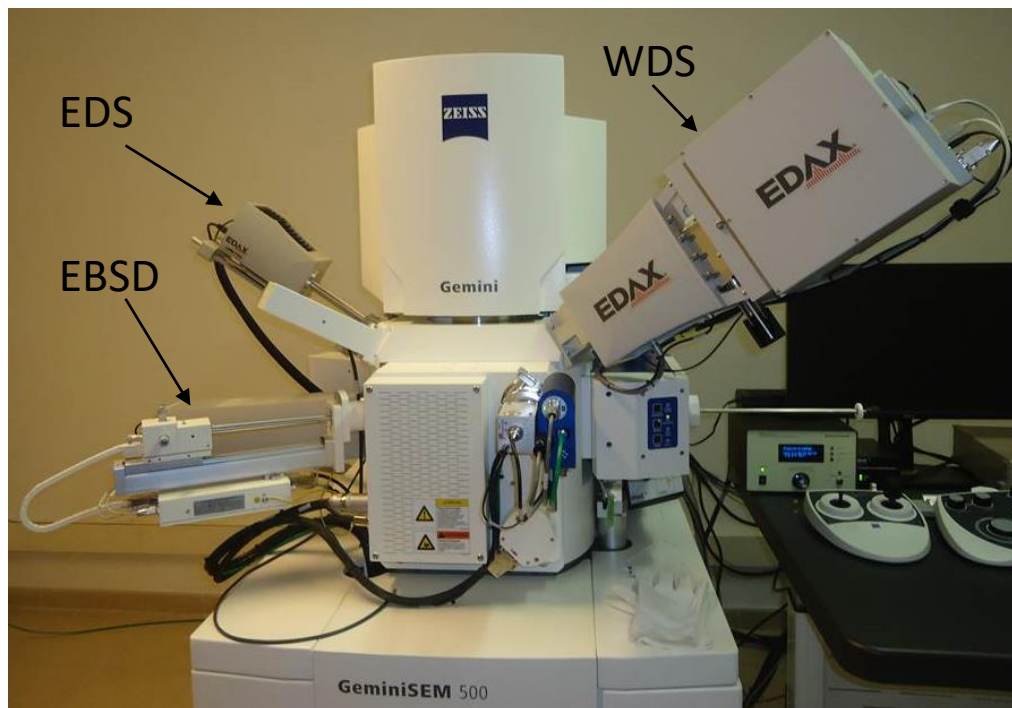
Martiane Cabié, Thomas Neisus

Sommaire

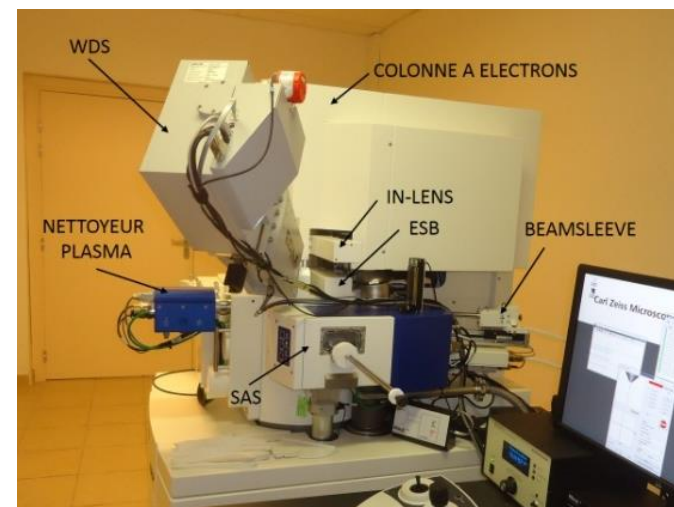
- Système MEB
- Tokamak WEST
- Dépôts
- Poussières
- Conclusion et perspectives

Février 2015

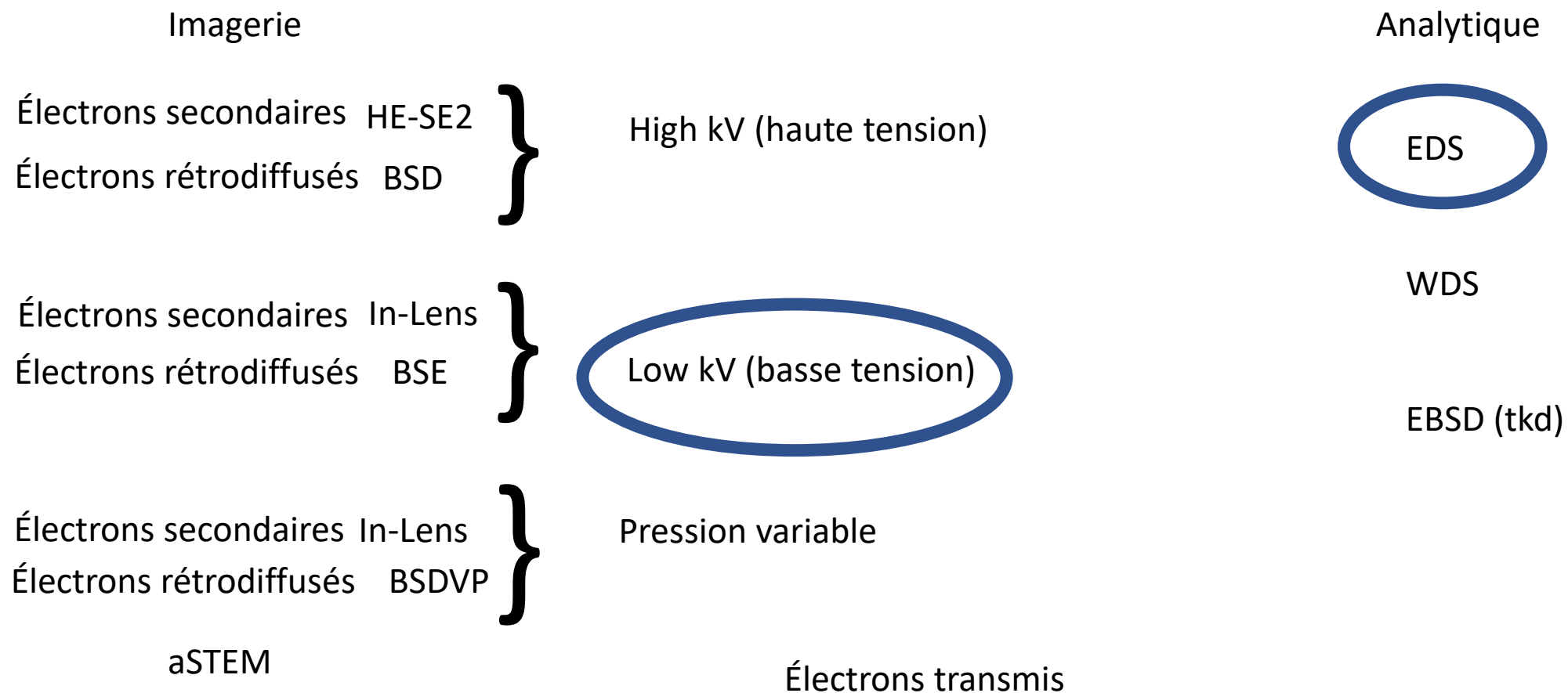
MEB ZEISS Gemini 500 20 nA



Resolution	1.2 nm (500 V)	1.8 nm (3kV, 50 Pa VP)
	1.1 nm (1 kV)	
	0.6 nm (15 kV)	0.9 nm (1kV, Sample Bias)
Beam Current	3 pA (1 kV) - 20 nA (30kV), 2 Gun Modes, 14 Steps	
Variable Pressure	5 – 500 Pa high resolution configuration	
	5 – 150 Pa large field of view configuration	



Avec un système doté de 7 détecteurs pour l'imagerie et 3 détecteurs de techniques analytiques, il est possible de caractériser une vaste gamme de matériaux en synergie avec d'autres techniques comme TEM, DRX, AFM, RAMAN.



SmartSEM - [CP2M]

File Edit View Beam Detection Image Scanning Stage Vacuum Tools Help

1 2 3 4 5

EDS

WDS

STEM

ZEISS 2 μm Gemini SEM 500 70-04

EHT = 20.00 kV	Mag = 4.00 K X	Noise Red. = Pixel Avg.	22 Nov 2016
WD = 11.9 mm	Pixel Size = 27.91 nm	Scan Speed = 3	11:14:45
Signal A = USB TV1	B = 64.9 % C = 79.8 %	Cycle Time = 399.55 ms	CP2M
		P = 6.31e-007 mbar	
		Ap. Size = 120.0 μm	

Gemini SEM Control

Control Imaging Gun Vacuum Stage

Status

EHT = 20.00 kV

Extractor V = 4.25 kV

Ext I Monitor = 372.7 μA

Fil I = 2.310 A

☒ Leave Gun On at Shutdown

☒ EHT Off @ Log Off

Fil I Target = 2.310 A

Extractor V Target = 4.25 kV

High Res Gun Mode Analytic Gun Mode

Optiprobe

☒ OptiProbe

OptiProbe Status = Ready

I Probe = 17.1 nA

Histogram

Specimen Current Monitor

Specimen I = -0.3 pA

SCM Status = Valid

☒ Stage Bias ☐ Spot

☐ Touch Alarm Disable

Ready.

Left: Brightness = 64.9 % | Mid: Contrast = 79.8 % | WD = 11.9 Fine All: ☒

Le contexte → <https://irfm.cea.fr/presentation-de-west/>

ITER est l'acronyme de **International Thermonuclear Experimental Reactor** en anglais, qui signifie « le chemin » en latin. Par extension, le sigle ITER désigne à la fois le réacteur et l'organisation en charge du projet.

ITER nécessite un composant essentiel, **le divertor**, qui reçoit la majeure partie du flux de chaleur et des particules provenant du plasma central pendant les expériences.

Dans le cadre du projet **WEST (Tungsten Environment in Steady State Tokamak)**, cela consistait à installer et à tester un tel divertor dans un autre tokamak : Tore Supra, une installation expérimentale unique en son genre grâce à ses aimants supraconducteurs et à ses composants activement refroidis en contact avec le plasma.

La configuration magnétique de Tore Supra a donc été modifiée, transformant sa forme circulaire en une lentille déformée, afin d'obtenir des plasmas aux caractéristiques similaires à celles d'ITER.

Le tokamak WEST permet aux chercheurs de mener un programme scientifique pertinent pour ITER, en se concentrant sur la préparation de l'exploitation d'ITER.

Afin de cartographier l'empreinte plasma complexe observée sur le divertor inférieur de l'expérience WEST après sa première phase de fonctionnement, nous avons analysé des dépôts prélevés sur des unités de contact plasma de type ITER (PFUs) exposées lors des campagnes C3 (plasma de deutérium) et C4 (plasma de deutérium et d'hélium)

Physica Scripta

PFU



PAPER

OPEN ACCESS

First post-mortem analysis of deposits collected on ITER-like components in WEST after the C3 and C4 campaigns

RECEIVED

25 June 2021

REVISED

6 September 2021

ACCEPTED FOR PUBLICATION

14 September 2021

PUBLISHED

28 September 2021

Céline Martin¹ , Mathilde Diez² , Andrea Campos³, Martiane Cabié³, Gregory Giacometti¹, Martin Balden⁴ , Alberto Gallo² , Bernard Pegourié², Elodie Bernard², Emmanuelle Tsitrone² the WEST team⁵

¹ Aix-Marseille University, CNRS, PIIM UMR 7345, Marseille, France

² CEA, IRFM, F-13108, Saint-Paul-Lez-Durance, France

³ Aix-Marseille University, CNRS, Centrale Marseille, FSCM, CP2M, Marseille, France

⁴ Max-Planck-Institut für Plasmaphysik, Boltzmannstr. 2, 85748 Garching, Germany

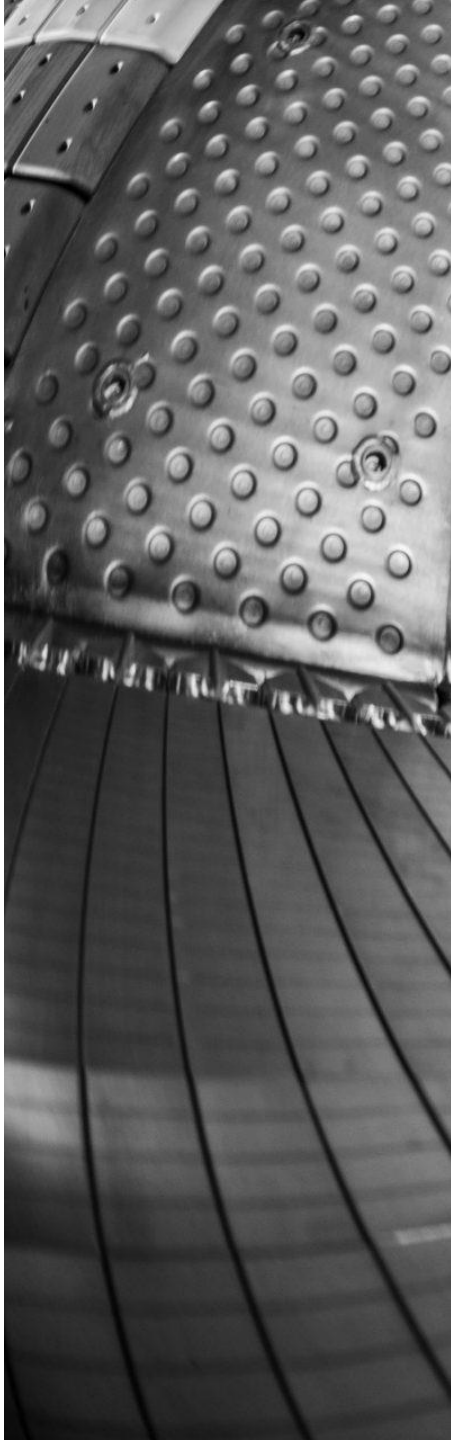
⁵ See <http://west.cea.fr/WESTteam>.

E-mail: celine.martin@univ-amu.fr

Keywords: WEST, divertor, erosion, redeposition, helium, boronization, TEM

Original content from this work may be used under the terms of the [Creative Commons Attribution 4.0 licence](#).

Any further distribution of



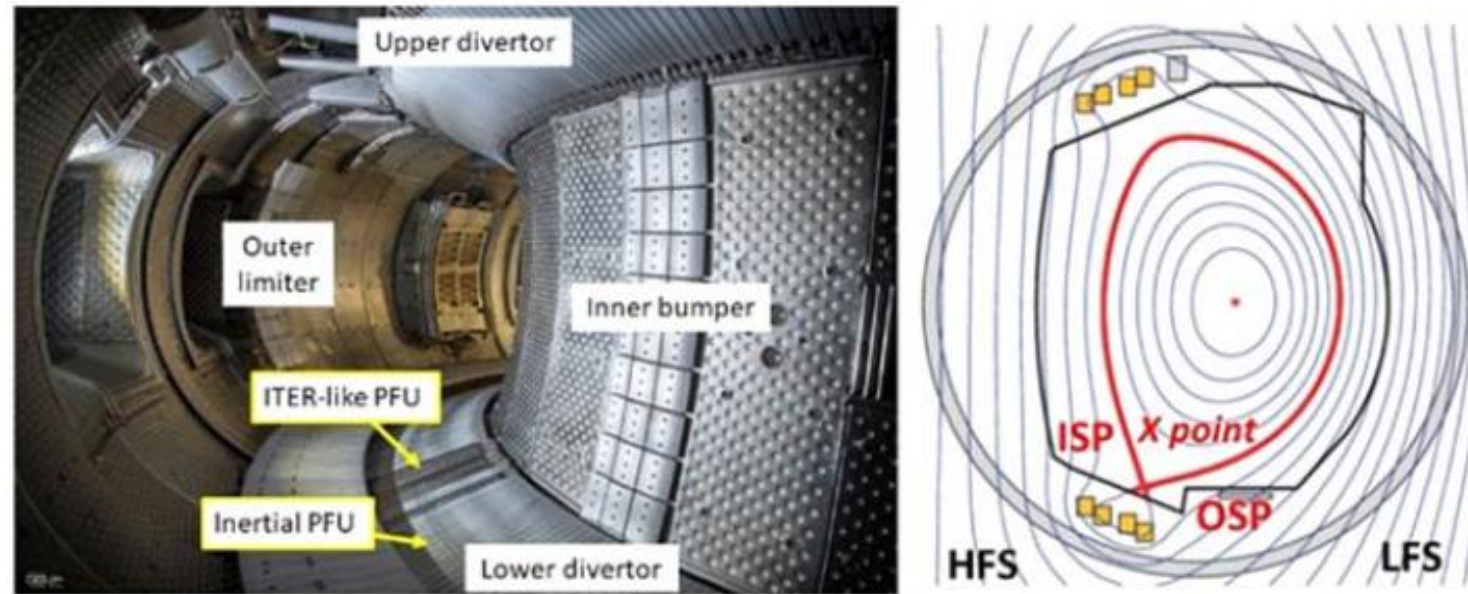


Figure 1. Photograph of the WEST vessel during phase 1 operation (before the start of the C3 campaign in 2018), showing the lower divertor equipped with a mix of ITER like actively cooled bulk W PFU and inertial W coated PFU. Typical magnetic equilibrium in WEST, showing the inner and the outer strike points located on the same target is depicted in the right hand side of the figure.

Boronise your Tokamak

📅 December 10, 2024 | 📧 Alberto Gallo (CEA) And Volker Rohde (IPP) | 📰 EUROfusion News

By layering the plasma-facing components of a fusion experiment with a thin layer of boron, fusion researchers boost the performance of their experiments and reduce the amount of impurities coming from the walls.

Tokamaks are at the forefront of nuclear fusion research, serving as experimental devices designed to achieve controlled thermonuclear fusion. By confining hot plasma using powerful magnetic fields, tokamaks aim to replicate the energy production processes found in stars, potentially offering a virtually limitless and clean energy source.

To maintain optimal plasma conditions and performance, researchers employ special techniques to condition the walls of their machines. These techniques are essential in reducing impurities that can cool the plasma and degrade its performance. Among these, boronization stands out as a particularly effective method. By depositing a thin boron layer on the plasma-facing components, boronization significantly reduces impurities and enhances plasma performance.

Boronization

The boronization process involves a glow discharge, similar to the effect seen in neon tubes, during which a boron-rich gas such as diborane is introduced into the tokamak. This gas decomposes and deposits a boron-hydride layer on the inner wall of the machine. Different boronization techniques include glow discharge boronization and Ion Cyclotron Range of Frequencies (ICRF) boronization.

In terms of plasma exposure, the C3 campaign was the first campaign with significant cumulated plasma duration (~2 h of deuterium (D) plasma exposure, to be compared with less than ~30 min for C1 and C2) and power coupled to the plasma (up to ~5 MW of Lower Hybrid (LH) power for C3, to be compared with 2.5 MW for C1-C2). **First boronizations were performed in C3 (3 boronizations).** In the C4 campaign, the coupled power was raised up to 9 MW of combined LH and ICRH power, and both D and helium (He) operation were performed, with more than 2.5 h of D exposure and ~45 min of He exposure.

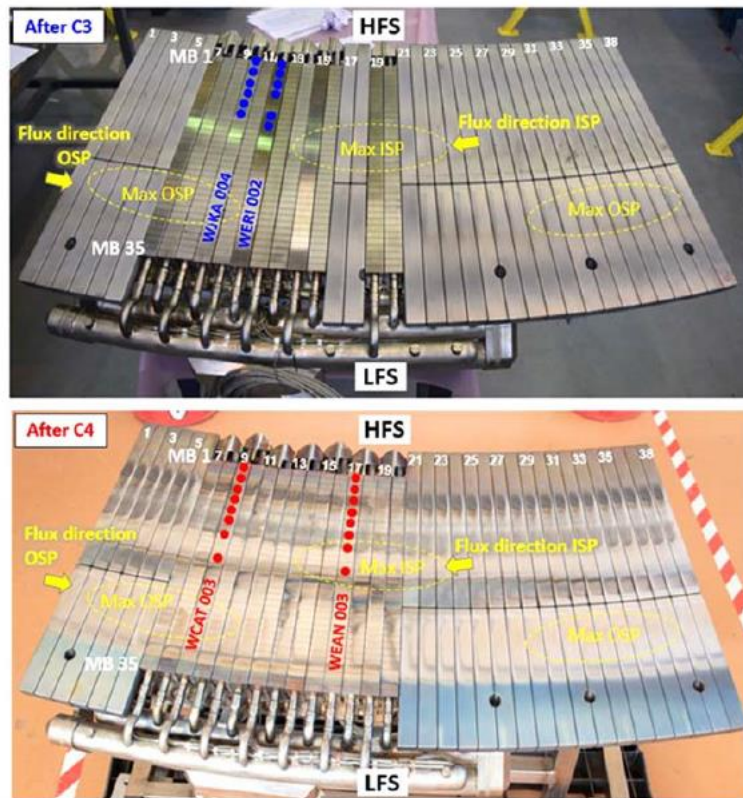




Figure 2. Configuration of the WEST test divertor sector for the C3 campaign with 12 ITER like PFU (top) and for the C4 campaign with 14 ITER like PFU (bottom). The PFU numbering on the sector (from 1 to 38) is indicated as well as the PFUs where the deposits have been collected after the C3 and C4 campaigns. Finally the areas of maximum plasma loads alternating on the HFS (max ISP) and LFS (max OSP) due to the impact of the magnetic ripple are shown.

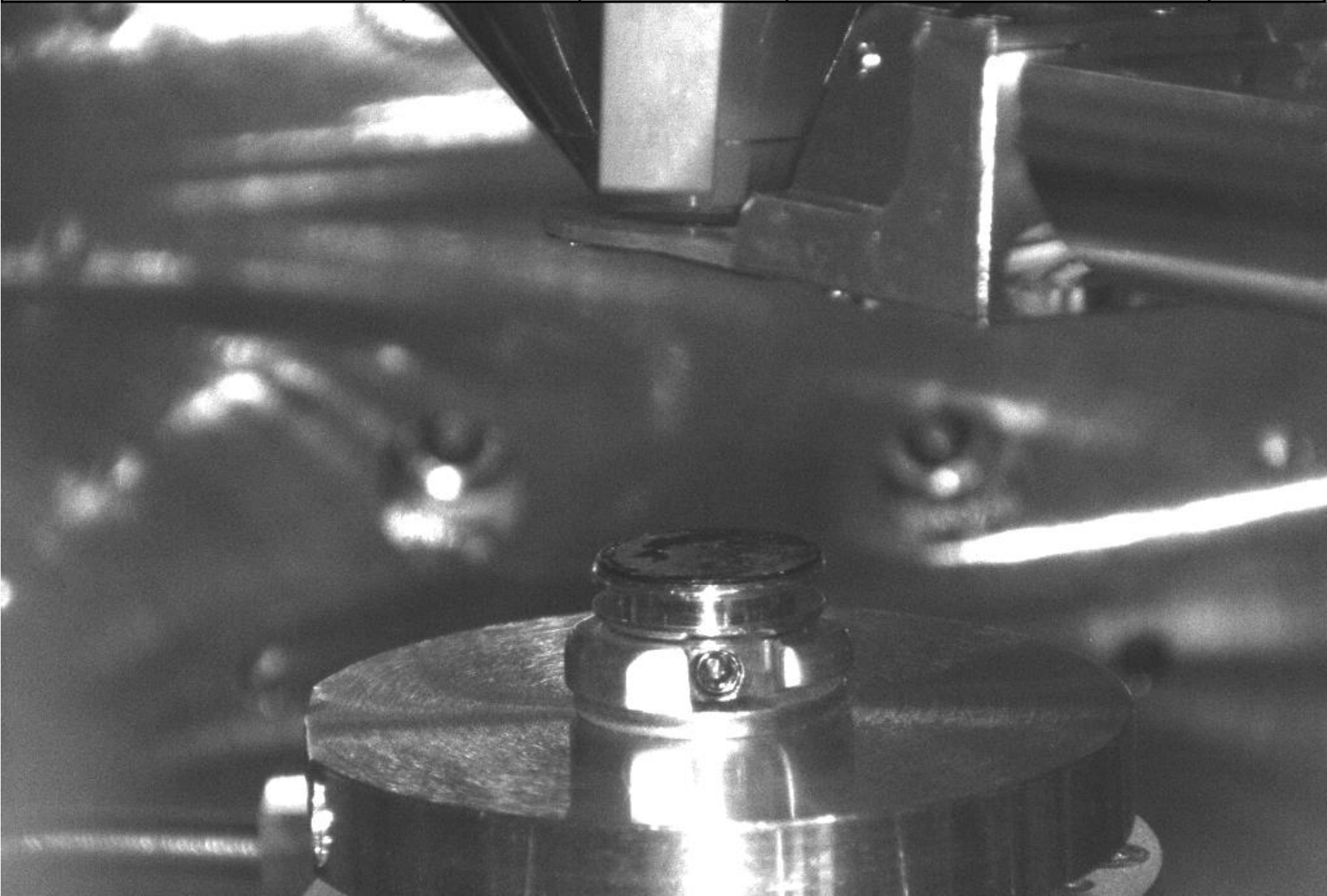
Plot MEB avec
Scotch carbone
double-face




Figure 3. Photograph of PFU WEAN003 taken after the deposits have been collected using the SEM holder. Inset showing a photograph of the SEM sample holder with the deposit on the carbon tape. The table below details the MB's where deposits have been collected for each PFU.


Les dépôts ont été analysés par microscopie électronique à balayage (MEB, Zeiss Gemini SEM500) couplée à un détecteur à dispersion d'énergie des rayons X (EDAX SDD). Des images en électrons rétrodiffusés (BSE) ou en électrons secondaires (SE) ont été acquises pour mettre en évidence le contraste chimique ou topographique. Les spectres ont été enregistrés pendant 200 secondes avec une **énergie incidente de 5 kV** pour la détection de B, W, C et O, et de 15 kV pour la détection de traces métalliques

 <div data-bbox="458 0 891 142"><p>200 μm</p><p>Gemini SEM 500 70-04</p></div>	<p>EHT = 15.00 kV WD = 18.7 mm Signal A = USB TV1</p>	<p>Mag = 70 X Pixel Size = 1.595 μm B = 59.5 % C = 100.0 %</p>	<p>Noise Red. = Pixel Avg. Scan Speed = 3 Cycle Time = 378.66 ms</p> <p>P = 4.30e-06 mbar Ap. Size = 60.00 μm</p>	<p>22 Mar 2021 16:34:51</p>
---	---	---	--	---------------------------------



 <div data-bbox="458 14 560 71">200 μm</div> <div data-bbox="458 92 764 128">Gemini SEM 500 70-04</div>	EHT = 15.00 kV WD = 50.0 mm Signal A = HE-SE2	Mag = 28 X Pixel Size = 3.987 μm B = 14.6 % C = 35.3 %	Noise Red. = Pixel Avg. Scan Speed = 7 Cycle Time = 5.3 Secs P = 5.61e-06 mbar Ap. Size = 60.00 μm	19 Nov 2020 10:01:03
--	---	---	---	-------------------------

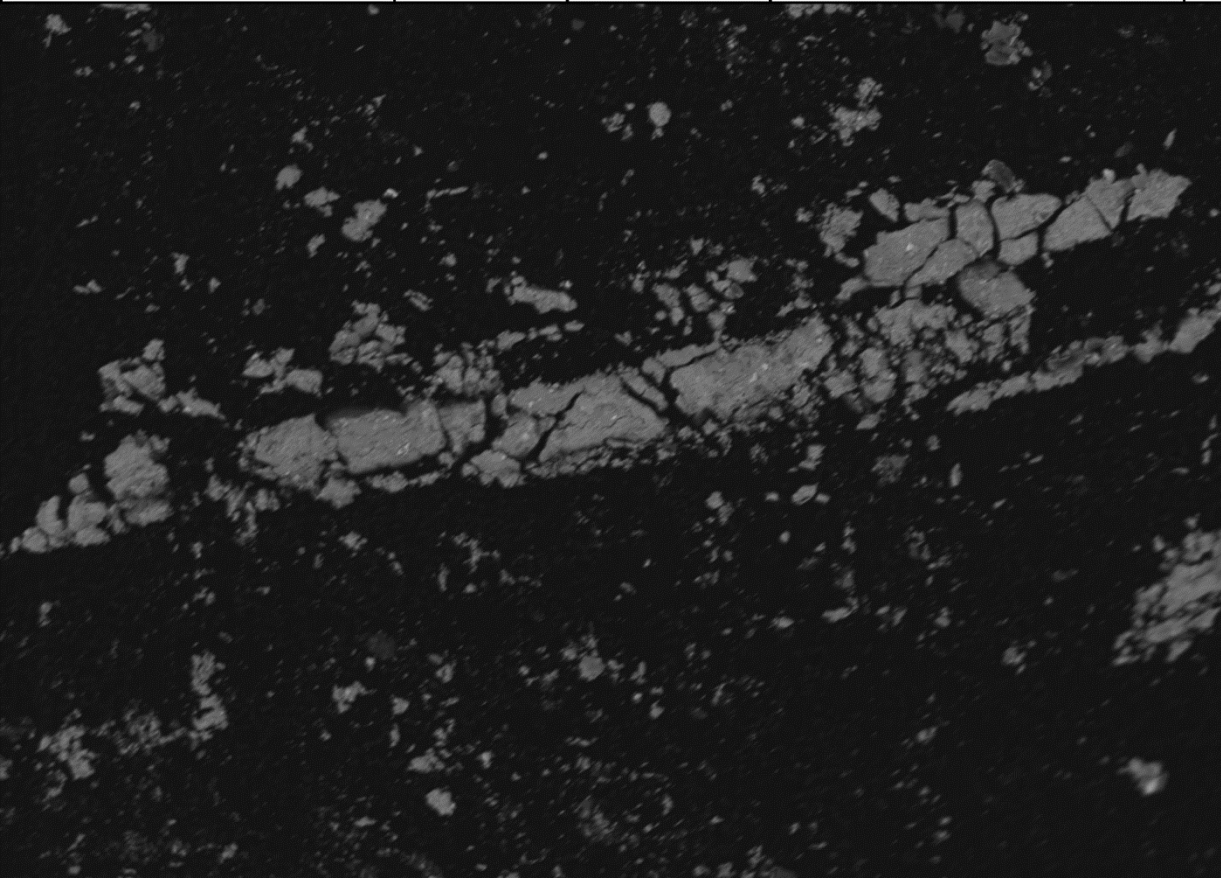





10 μ m

Gemini SEM 500 70-04

EHT = 5.00 kV	Mag = 1.36 K X	Noise Red. = Pixel Avg.	19 Nov 2020
WD = 11.8 mm	Pixel Size = 41.05 nm	Scan Speed = 8	14:02:49
Signal A = BSD4 A	B = 40.7 % C = 10.2 %	Cycle Time = 40.7 Secs	Ap. Size = 120.0 μ m

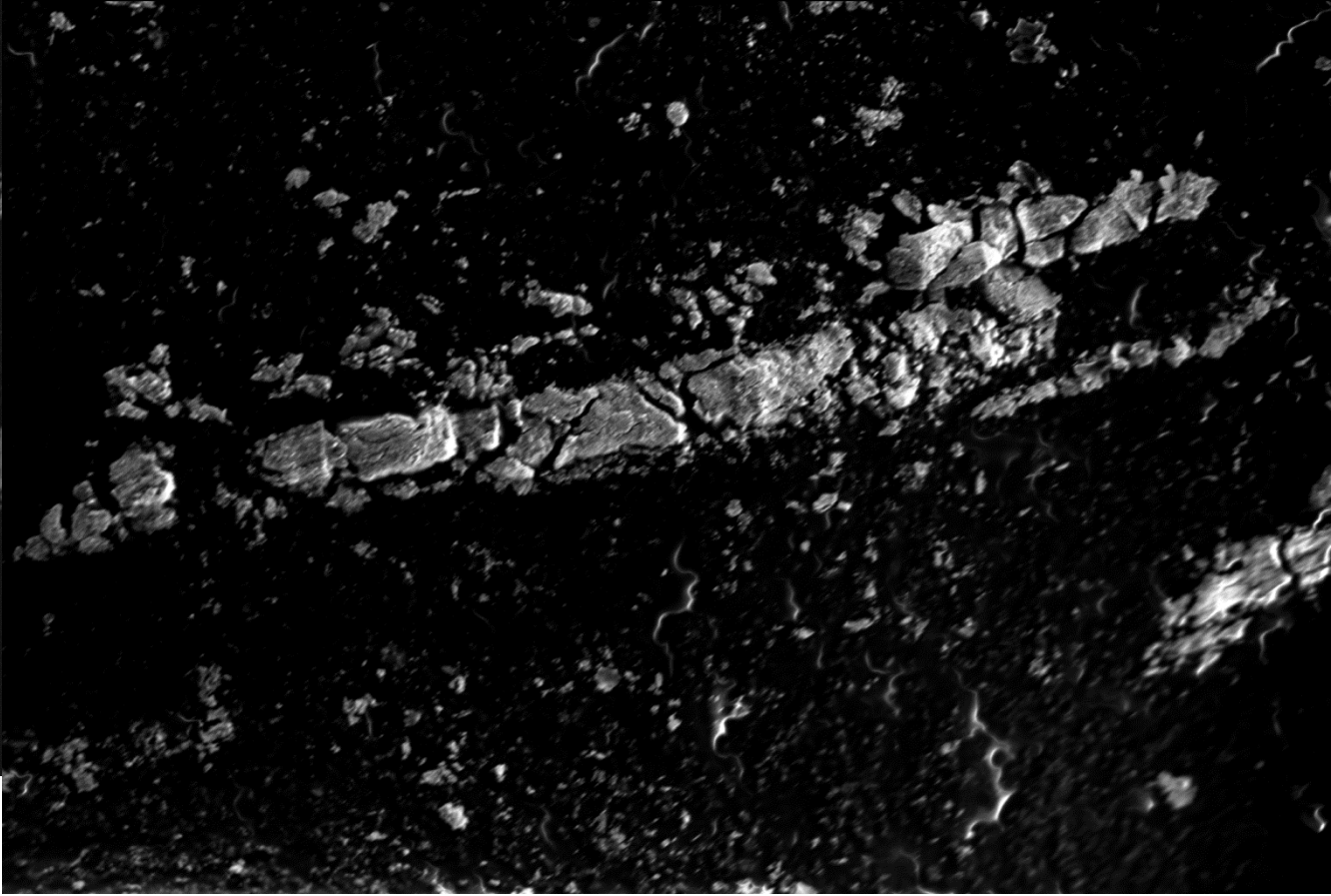


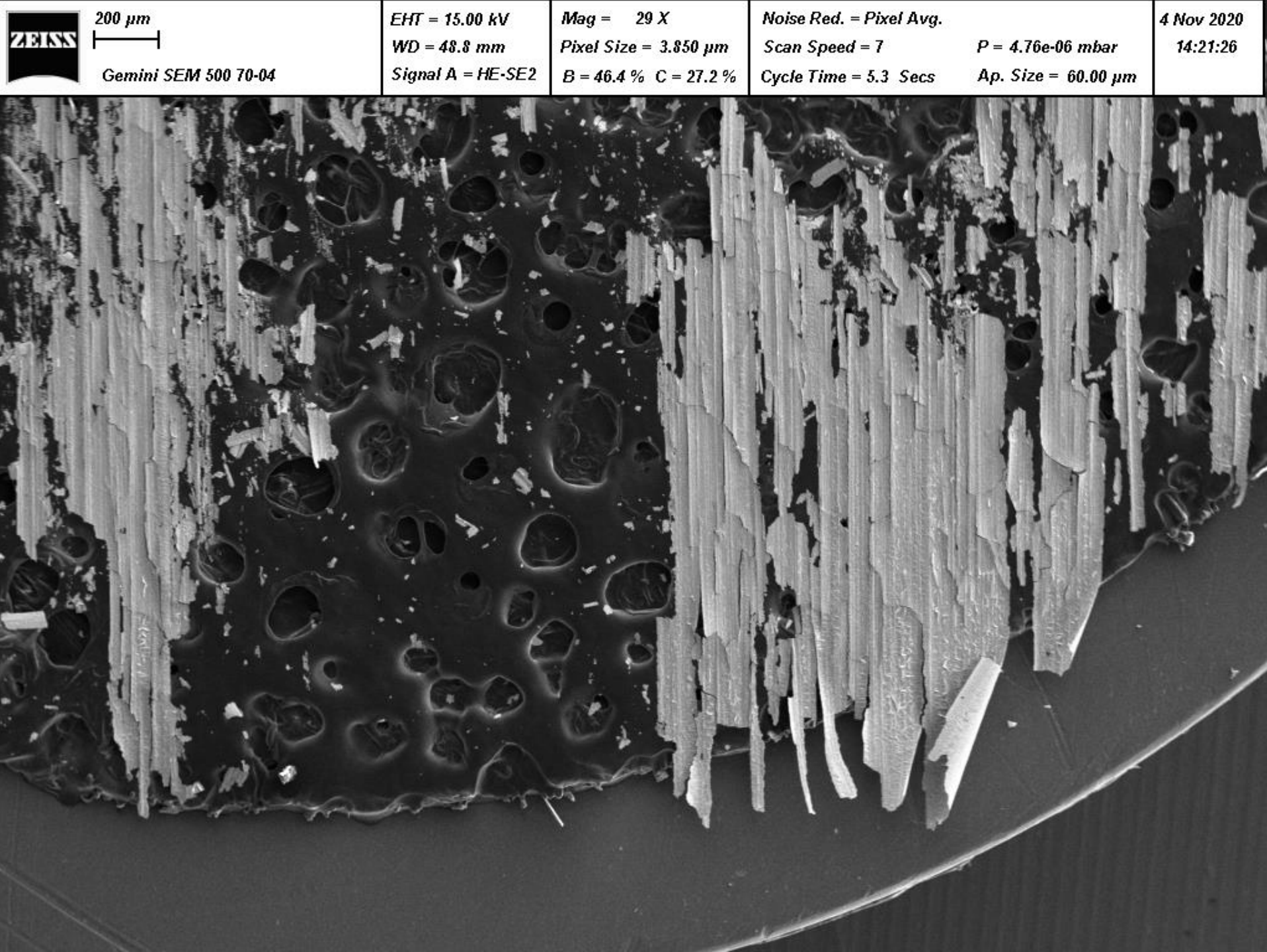


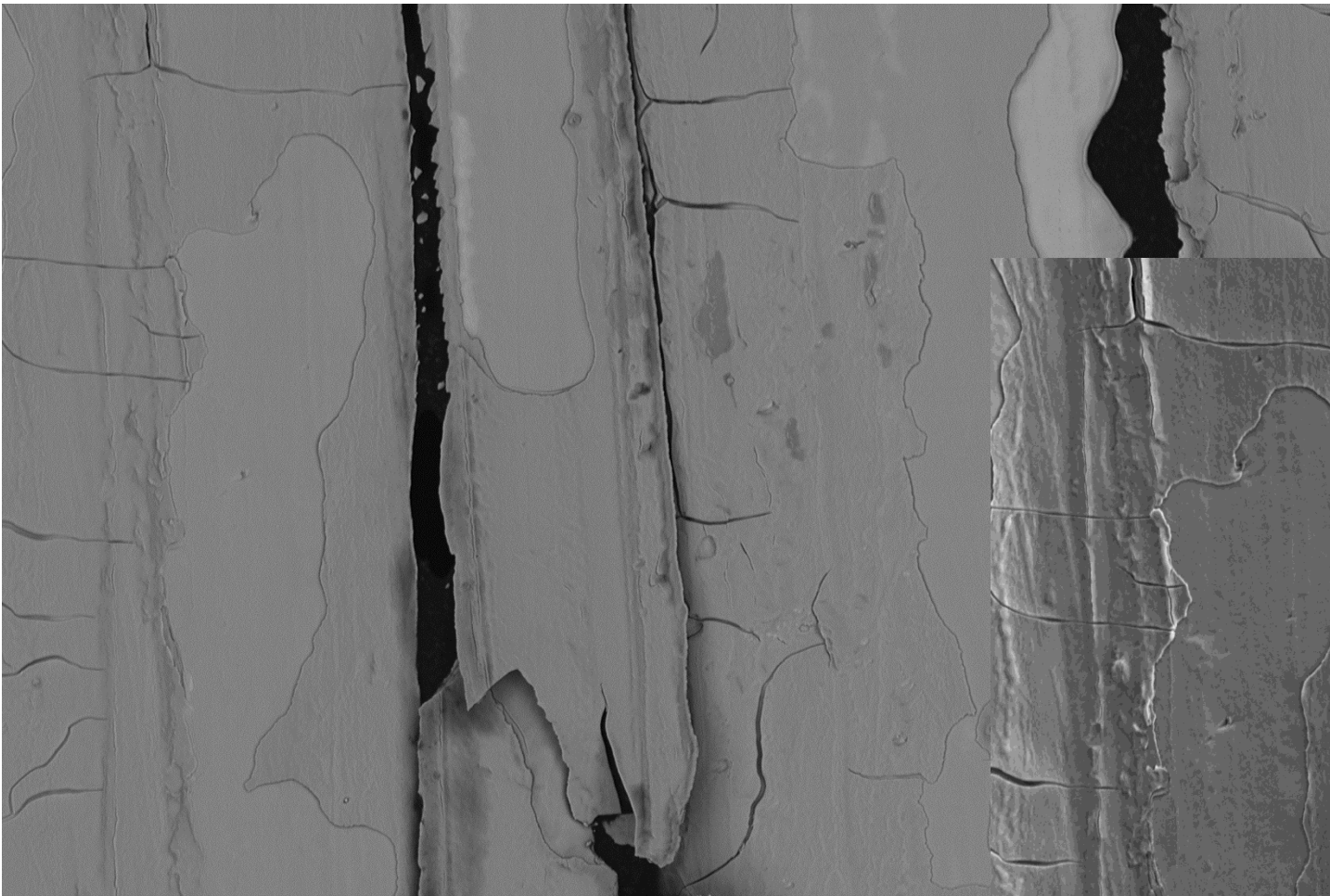
10 μ m


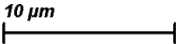
Gemini SEM 500 70-04

EHT = 5.00 kV	Mag = 1.36 K X	Noise Red. = Pixel Avg.	19 Nov 2020
WD = 11.8 mm	Pixel Size = 41.05 nm	Scan Speed = 8	14:02:49
Signal A = HE-SE2	B = 41.1 % C = 26.4 %	Cycle Time = 40.7 Secs	Ap. Size = 120.0 μ m


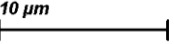
This SEM image shows a dark, granular surface with a prominent, bright, elongated feature that appears to be a fracture or a cluster of small, angular particles. The feature is roughly horizontal and spans the middle of the frame. The background is dark and textured with small, bright spots.





 Gemini SEM 500 70-04		EHT = 5.00 kV	Mag = 1.36 K X	Noise Red. = Line Int. B
		WD = 12.3 mm	Pixel Size = 41.05 nm	Scan Speed = 4
		Signal A = BSD4 A	B = 47.3 % C = 40.2 %	Cycle Time = 1.2 Mins



 Gemini SEM 500 70-04		EHT = 5.00 kV	Mag = 1.36 K X	Noise Red. = Line Int. Busy	4 Nov 2020 15:13:44
		WD = 12.3 mm	Pixel Size = 41.05 nm	Scan Speed = 4	
		Signal A = HE-SE2	B = 45.7 % C = 29.5 %	Cycle Time = 1.2 Mins	
				Ap. Size = 60.00 µm	

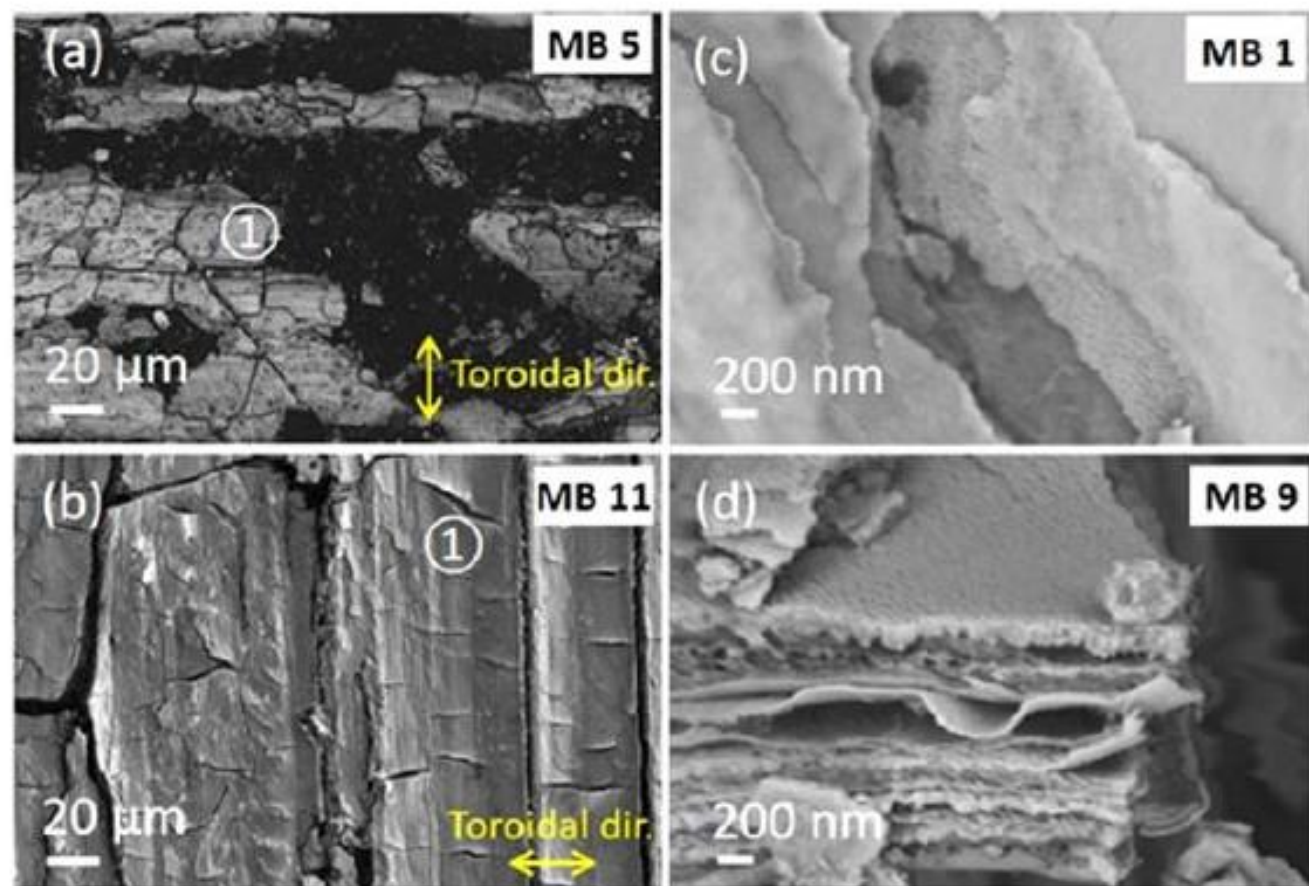
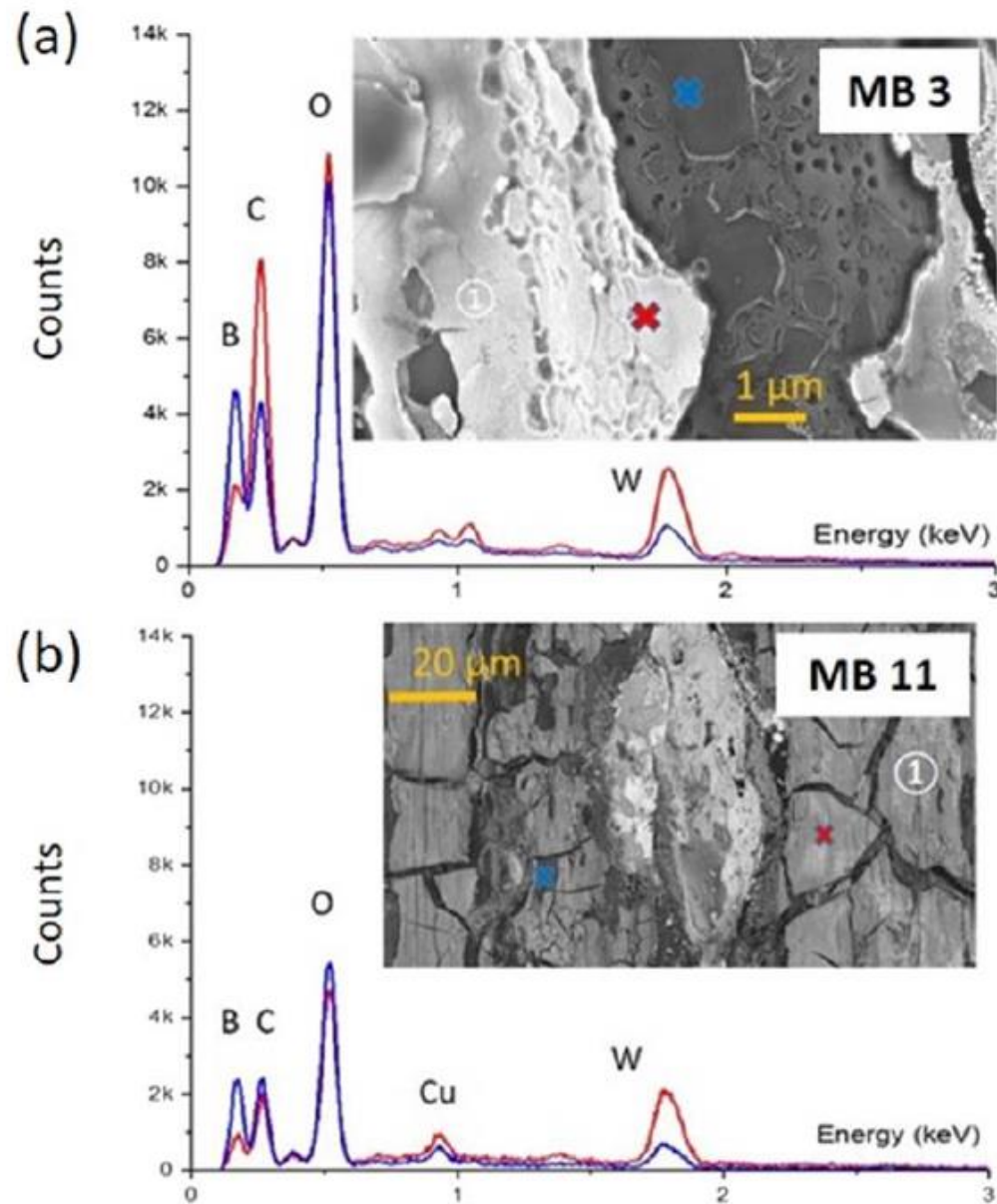


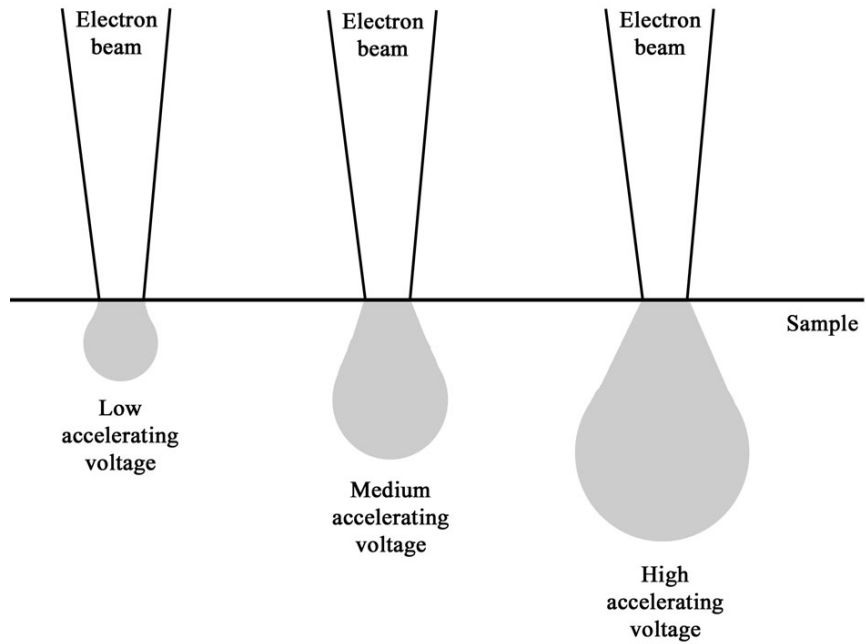
Figure 4. SEM images (BSE mode) showing the morphology of the deposits collected after the C3 campaign on (a) WERI002 MB 5 (b) WJKA004 MB 11 (SE mode for this image only). On the right hand side, high magnification images of WJKA004 (c) different textures found in the first layers of MB 1, (d) thin layers of different texture found in a deposit scrap observed by its section.



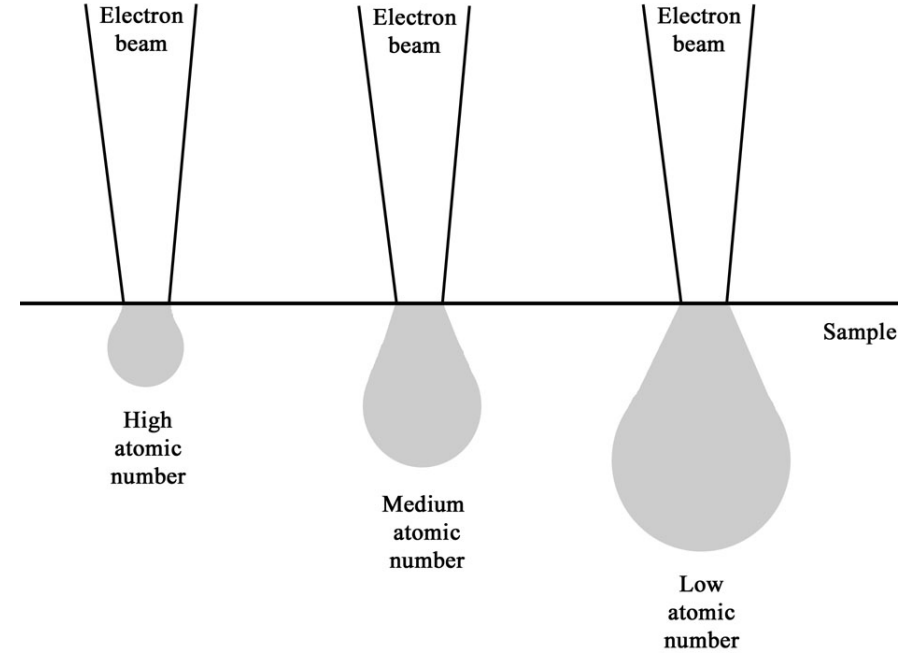
Choix de 5kV :
Observation des raie BK
et W M

Figure 7. EDX spectra of the first layer (red) and the underneath layer (blue) for deposits collected after C4 on WEAN003 (a) MB 7 (b) MB 11.

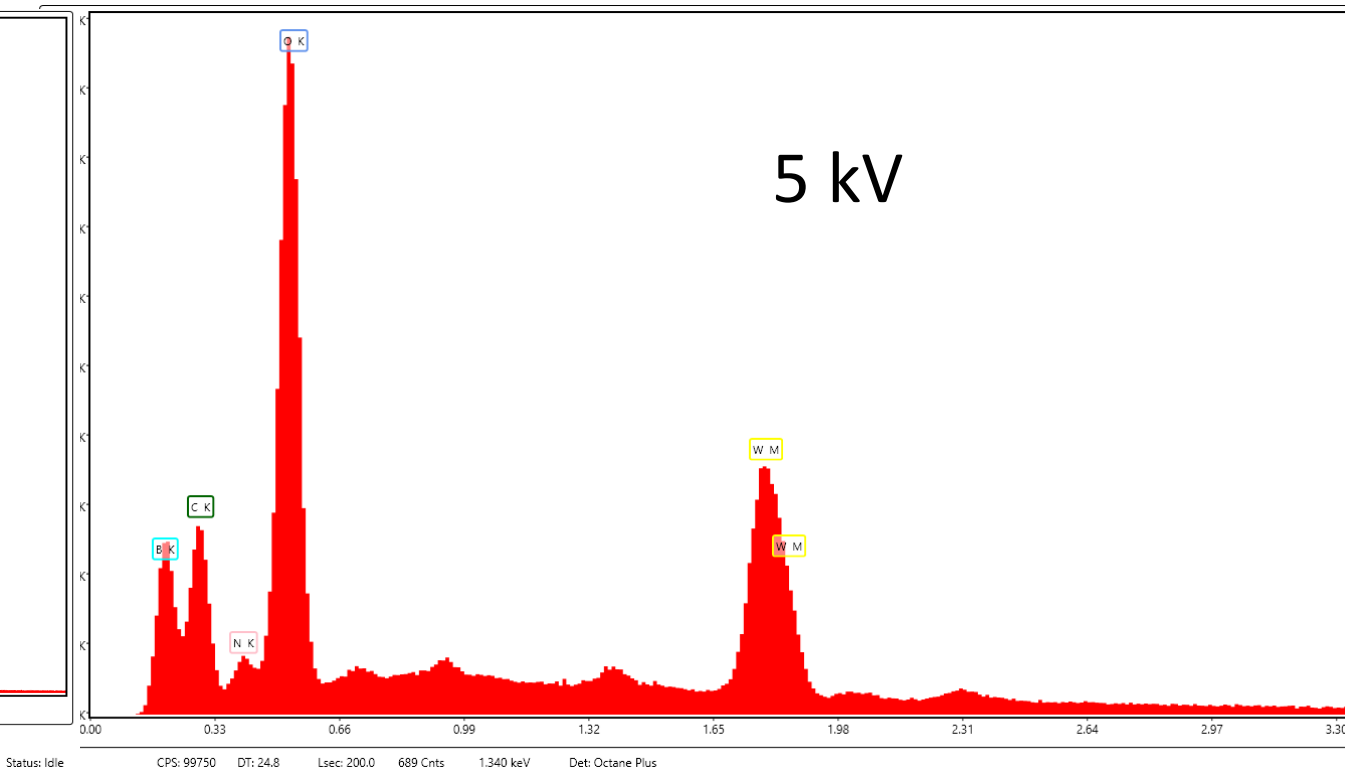
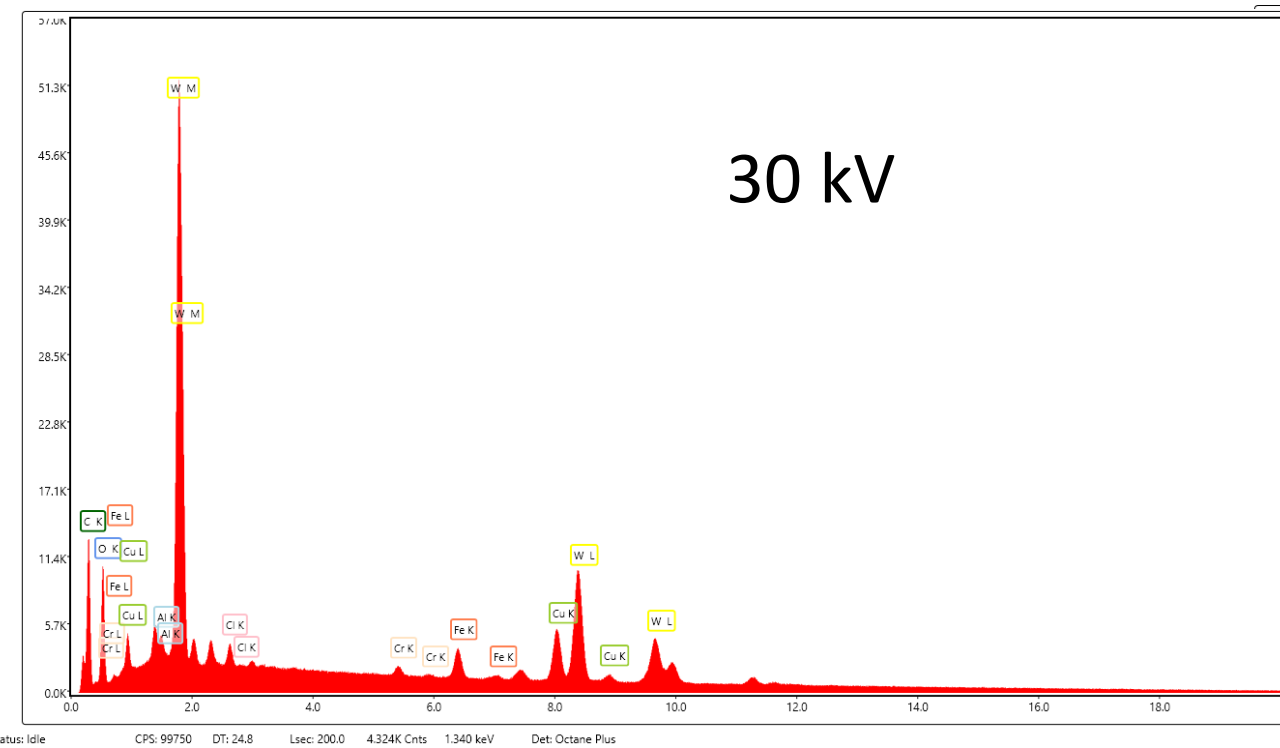
Influence de l'énergie primaire



Influence de la nature de l'échantillon



Choix de la basse tension



Les résultats MEB-EDX nous ont permis d'identifier trois types de dépôts associés à différentes zones sur la face interne du divertor inférieur.

Table 1. Adhesion, morphology and chemical composition of the deposits identified in the three locations of the lower divertor.

		After C3 campaign			After C4 campaign				
		Adhesion	Morphology	Composition			Adhesion	Morphology	Composition
Low flux	MB 1–7	strong medium	homogeneous rough and cracking figures 4(a) and 6(a)	B and C-rich layers figure 6(a)	MB 1–5	strong medium	homogeneous smooth and peeling off figures 5(a) and 7(a)	B and C-rich layers figure 7(a)	
High flux	MB 9–13	low	homogeneous smooth and peeling off figures 4(b) and 6(b)	W-rich layers no B and C figure 6(b)	MB 7–13	low	non homogeneous smooth and crack- ing figure 5(b)	W-rich area B and C-rich lay- ers figure 7(b)	
ISP/Private					MB 17	medium	Anisotropic figure 5(c)	W-rich B and C-rich	

Analyse des dépôts en fonction de la profondeur → FIB + STEM + EDS

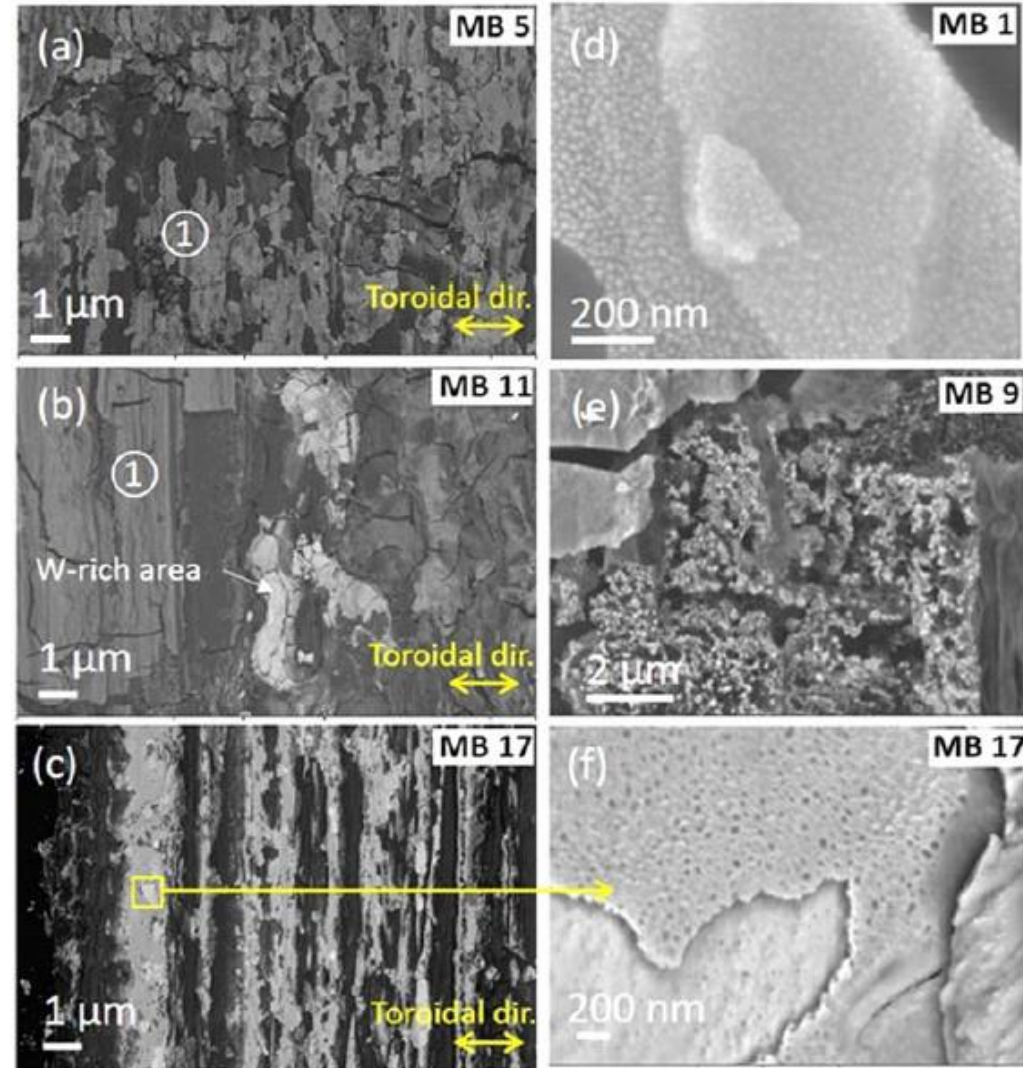
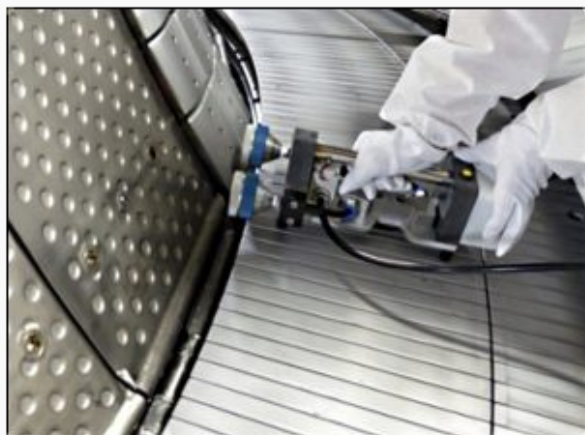


Figure 5. SEM images (BSE mode) showing the morphology of the deposits collected after the C4 campaign on WEAN003 (a) MB 5 (b) MB 11 and (c) MB 17. On the right hand side, high magnification images of (d) nanoparticles found in the first layer of MB 1, (e) particles in the underneath layer of MB 9 (f) nano-holes in a W-rich layer of MB 17.

[IRFM](#) > [Faits marquants](#) > Des nanoparticules de tungstène produites par les plasmas de tokamak



Des nanoparticules de tungstène produites par les plasmas de tokamak

Dans les machines de fusion, **les interactions du plasma avec les parois**, mais aussi les phases de maintenance, **peuvent produire des micro-débris ou poussières dans la chambre à vide** (une poussière est définie comme une matière particulaire d'une taille allant jusqu'à ~1mm)

11 octobre 2023

CATÉGORIES

Faits marquants

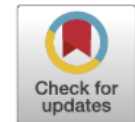
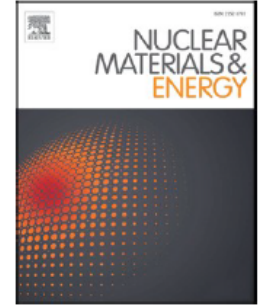


ELSEVIER

Contents lists available at [ScienceDirect](https://www.sciencedirect.com)

Nuclear Materials and Energy

journal homepage: www.elsevier.com/locate/nme



Micron-sized dust and nanoparticles produced in the WEST tokamak

C. Arnas^{a,*}, A. Campos^b, M. Diez^c, S. Peillon^d, C. Martin^a, K. Hassouni^e, A. Michau^e,
E. Bernard^c, N. Fedorczak^c, F. Gensdarmes^d, C. Grisolia^c, B. Pégourié^c, E. Tsitrone^c

^a CNRS, Aix-Marseille université, PIIM, 13397 Marseille, France

^b Aix-Marseille université, CNRS, Centrale Marseille, FSCM, CP2M, 13397 Marseille, France

^c IRFM/CEA Cadarache, 13108 St Paul Lez Durance, France

^d LPMA/IRSN, 91192 Gif-sur-Yvette, France

^e LSPM, CNRS, Université Paris 13, Sorbonne Paris Cité, 93430 Villetaneuse, France

Dans ce travail, nous présentons des exemples de particules de poussière produites lors des deux dernières campagnes plasma de la première phase de fonctionnement de WEST (C4-2019 et C5-2020).

Pendant les expériences, ces poussières peuvent être mobilisées, transportées dans le cœur du plasma pour devenir une source de pollution, avec pour conséquence de dégrader les performances du plasma et potentiellement entrainer son extinction.

il est essentiel d'appréhender au mieux les phénomènes de création de ces poussières dans des conditions aussi proches que possible de celles d'ITER.

Depuis 2017, des prélèvements sont réalisés dans l'enceinte à vide, au niveau du divertor, après chaque campagne expérimentale (et avant toute intervention humaine) dans le but de mieux comprendre les **mécanismes de formation**. Deux techniques sont utilisées pour la collecte des poussières : l'une utilisant une « duster box », dispositif conçu et mis à disposition, via une collaboration avec l'IRSN permettant de remettre en suspension et collecter les poussières présentes [1] (figure 1) et la seconde par une technique d'aspiration, via une collaboration avec le PIIM. Les poussières sont ensuite caractérisées par microscopie électronique au CP2M afin de révéler leur morphologie et leur composition chimique et de déterminer ainsi leurs origines possibles.

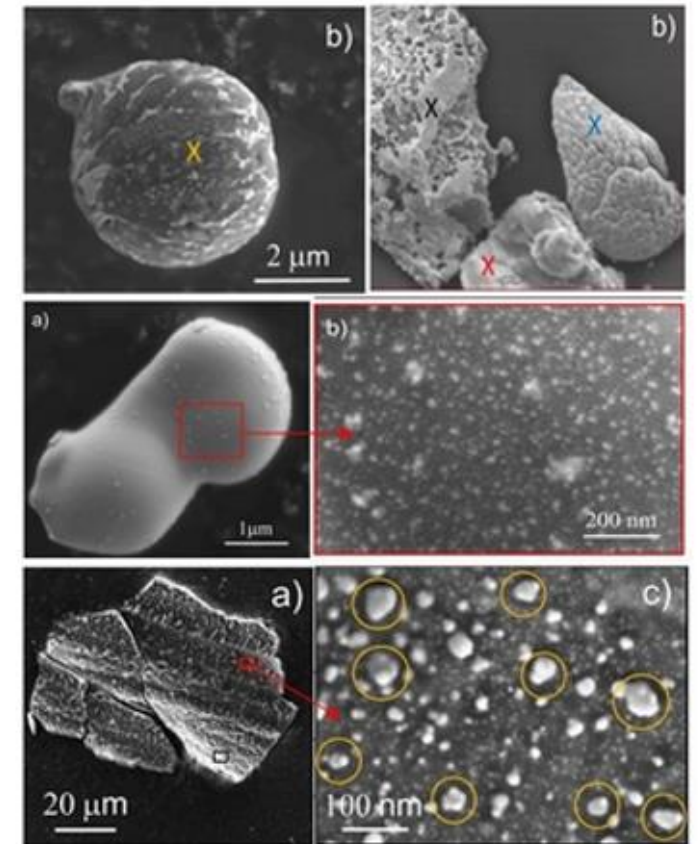
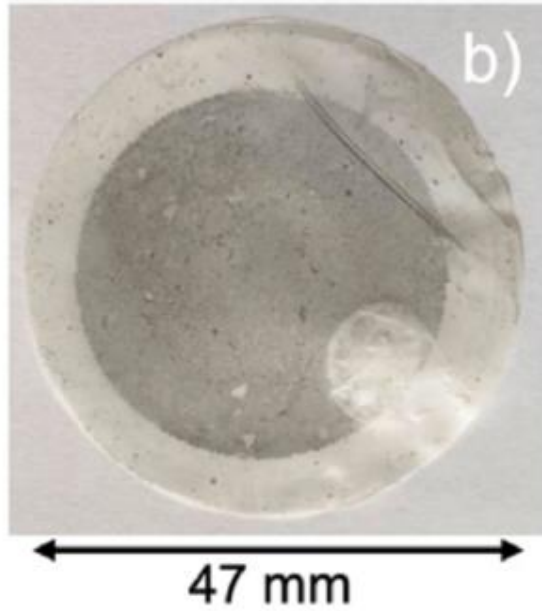


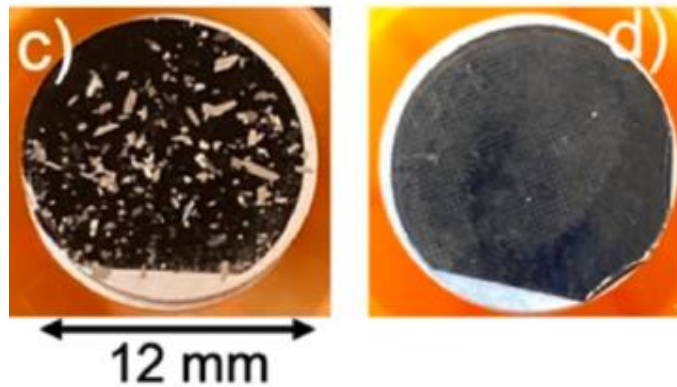
Figure 2 : examples of dust particles collected on the WEST divertor. Nanoparticles, separated or agglomerated, are visible on the surface of these dust particles; credit: Cécile Arnas, Andrea Campos;

Après la mise à l'air du réacteur et un contrôle de sécurité, la collecte de poussière a été effectuée sur le divertor inférieur en utilisant la technique de vide filtré



Pour les analyses MEB-EDS, les filtres ont été pressés contre des supports de microscope, recouverts de rubans adhésifs carbone double face, et les particules de poussière y ont été transférées

présence de deux populations distinctes de poussières après la campagne expérimentale de 2020.



Première population: poussières qui proviennent de la délamination des revêtements de tungstène, d'émission de gouttelettes de matériaux fondus suite à des charges thermiques intenses ou de la formation de particules de poussière dues à l'érosion des matériaux par le plasma.

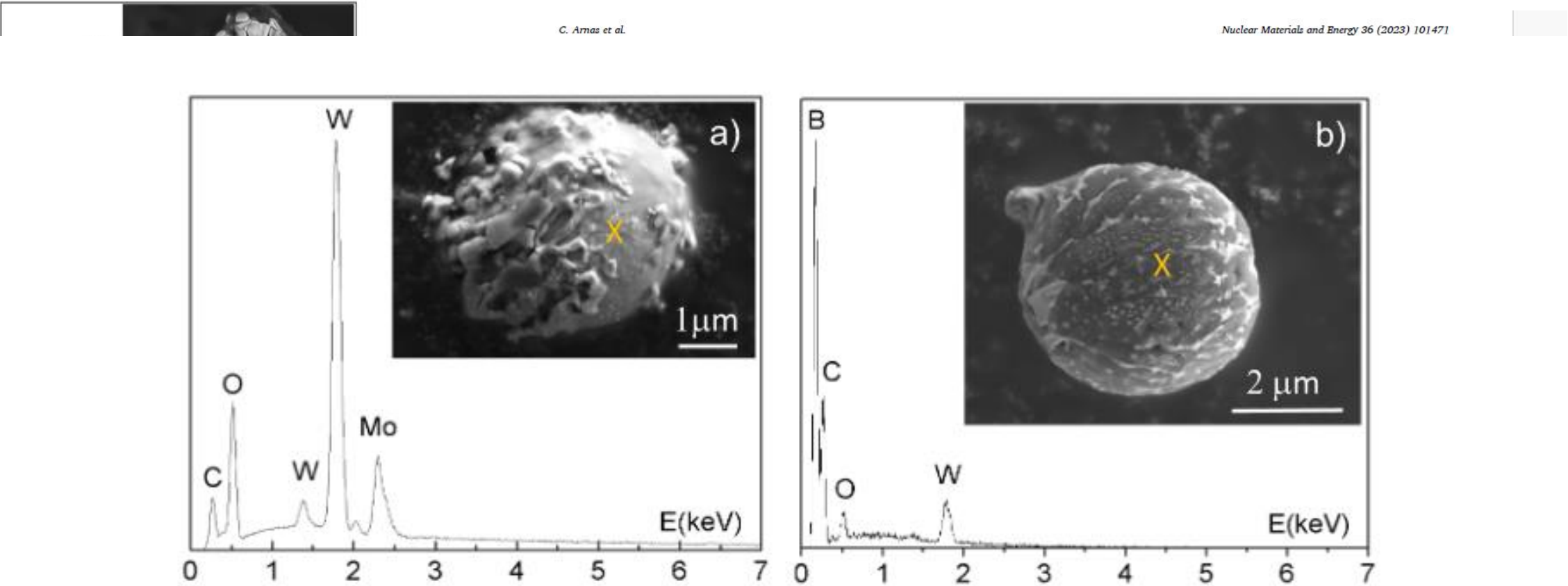
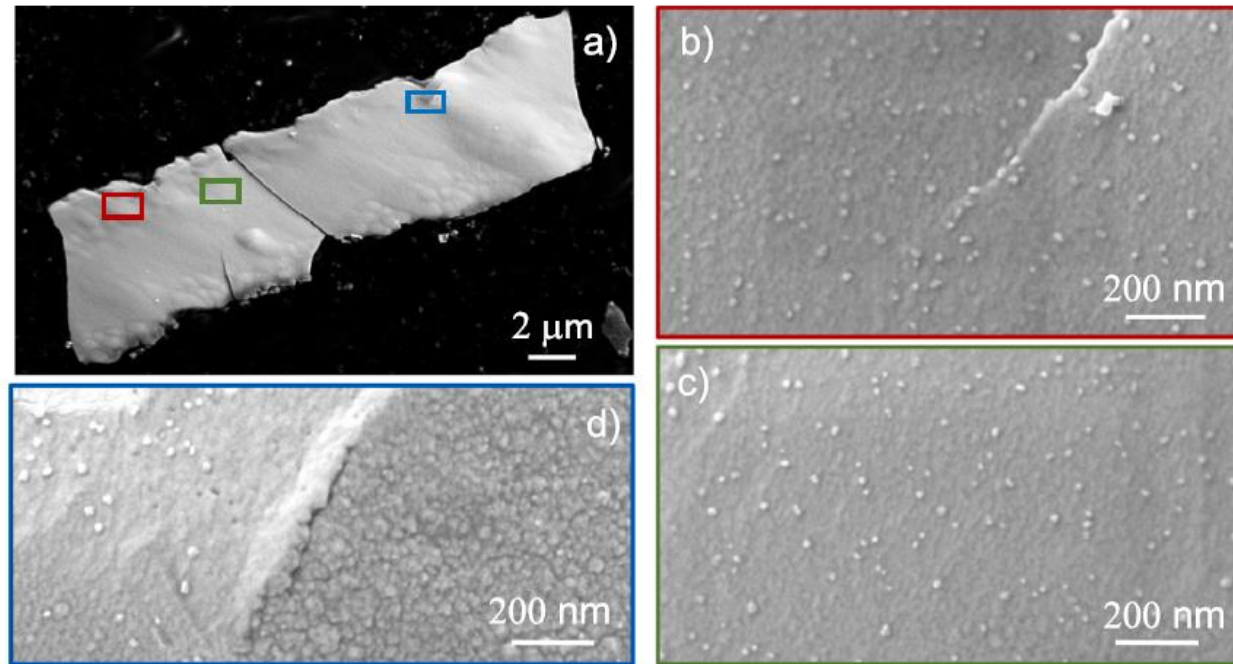


Fig. 4. a) W dominated spheroid containing C, O and Mo traces, size ~ 6 μm (C5 campaign). Molten W projections on the left side indicate that the dust temperature was close to that of a solid; b) B dominated spheroid containing C, O traces, size ~ 5 μm (C4 campaign). It was likely W before boronization.

image; C (in green) appears on other dark parts and the carbon adhesive tape around. (For interpretation of the references to colour in this figure legend, the reader is referred to the web version of this article.)

was close to that of a solid; b) B dominated spheroid containing C, O traces, size ~ 5 μm (C4 campaign). It was likely W before boronization.

2^{ème} population de poussières: nanoparticules de Tungstène.
Elles ont été trouvées essentiellement à la surface de particules de quelques μm et peuvent résulter soit de la condensation d'une vapeur sursaturée au-dessus du tungstène fondu, par exemple.



6. a) piece of W coating of $\sim 27 \mu\text{m}$ long and $\sim 8 \mu\text{m}$ wide (C4 campaign); b) and c) magnifications of the red and green squares of a) showing similar sizes, from 8 to 23 nm; d) detail of the blue square showing a smooth W area (left part) with dispersed NPs and a rough W area (right part). (For interpretation of the references to colour in this figure legend, the reader is referred to the web version of this article.)

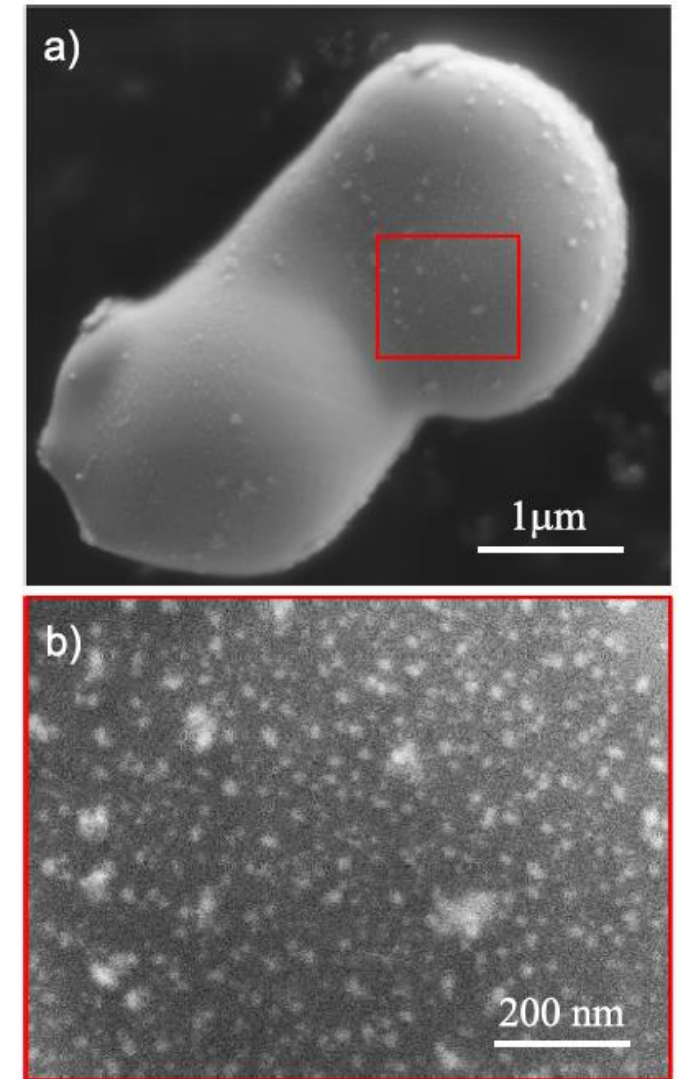


Fig. 7. a) two merged W droplets of size $\sim 2 \mu\text{m}$ each one (C4 campaign). NPs are present everywhere on the surface; b) magnification of the red square showing NPs of $\sim 20 \text{ nm}$ average size and few bigger ones. (For interpretation of the references to colour in this figure legend, the reader is referred to the web version of this article.)

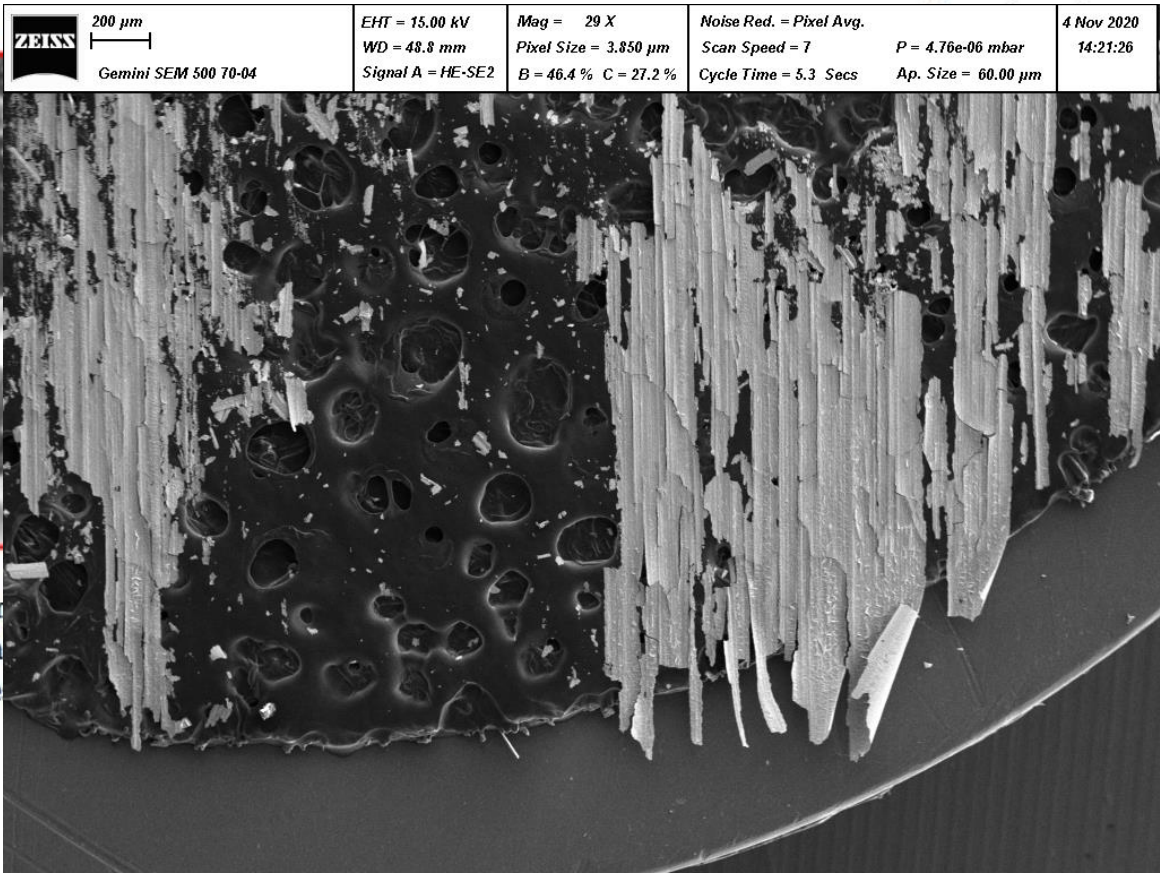
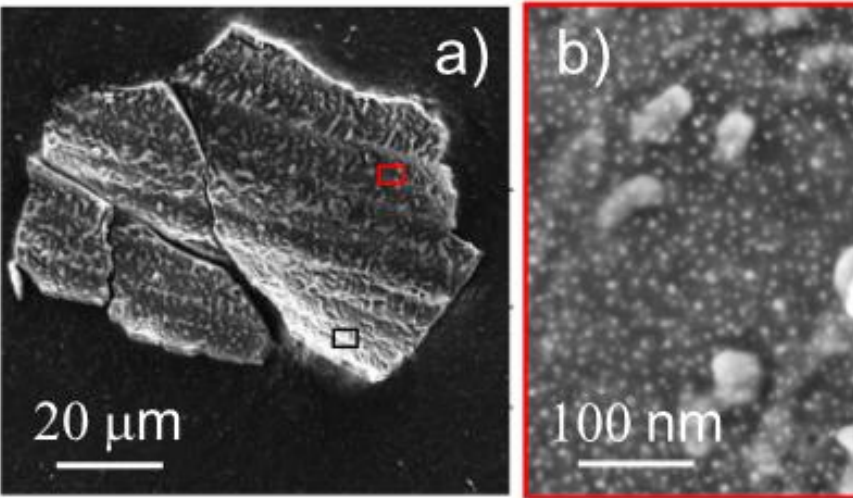


Fig. 8. a) piece of W coating of $\sim 90 \mu\text{m}$ long and $\sim 40 \mu\text{m}$ wide (C5 campaign square). Larger ones are either separated or melted with others to form chain background and bigger ones either separated or agglomerated (yellow circle referred to the web version of this article.)

Des nanocavités ont été trouvées à la surface des poussières de tungstène prélevées après une phase d'opération de WEST avec des plasmas d'hélium. Ceci peut être attribué au piégeage de l'hélium dans le tungstène sous forme de nanobulles, phénomène identifié en laboratoire et retrouvé en conditions tokamak.

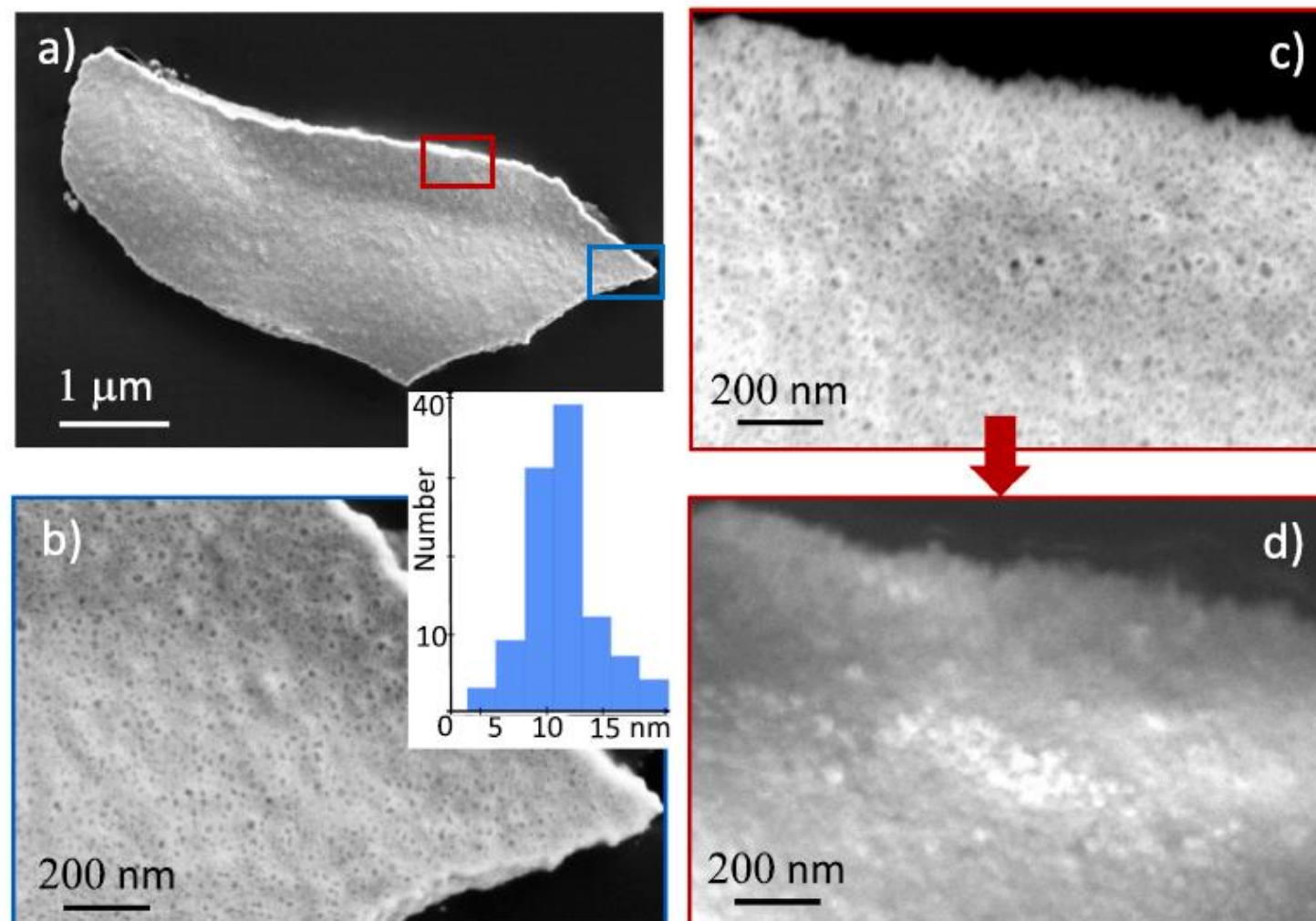
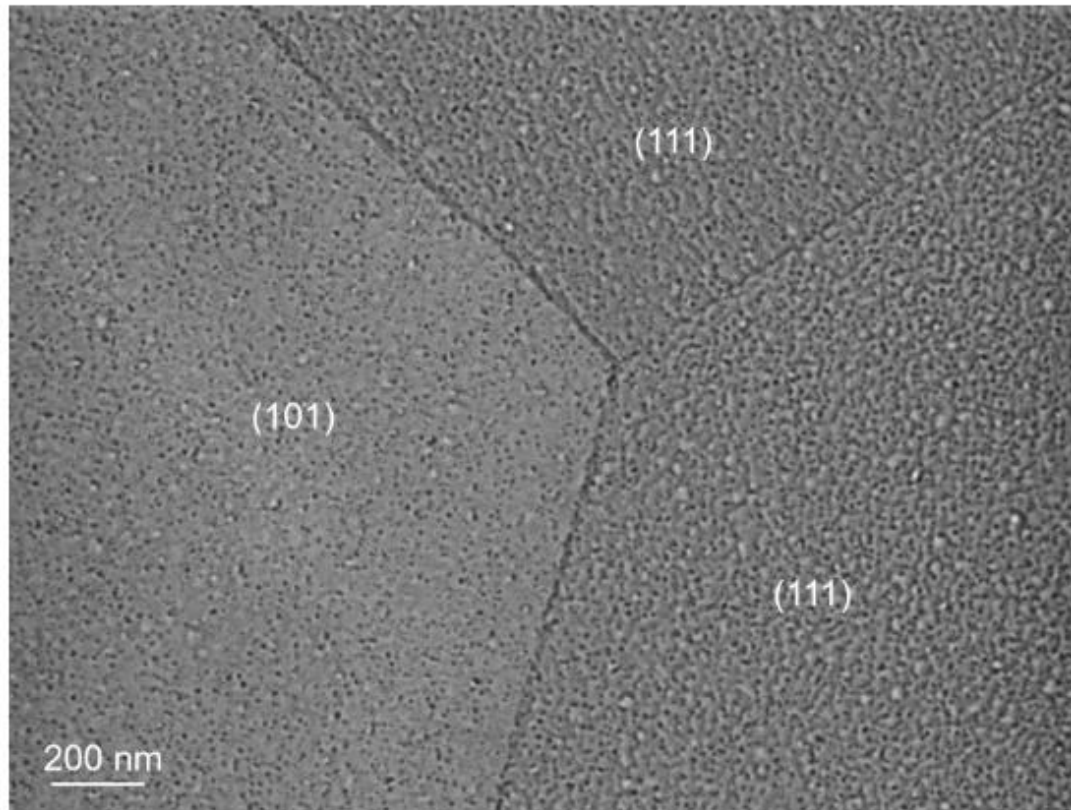


Fig. 9. a) piece of W coating of $\sim 5 \mu\text{m}$ long with nanoholes all over the surface (C4 campaign); b) size distribution (inset) of nanoholes of the dust tip; average size of 10.9 nm ; c) nanoholes in the red square of a); d) same area as c) revealing the presence of domes at the exact position of nanoholes in c), highlighting the presence of nanocavities produced by He nanobubbles. (For interpretation of the references to colour in this figure legend, the reader is referred to the web version of this article.)

Interaction W - Helium (irradiation au labo PIIM)



Grain orientation and temperature dependence of bubbles at tungsten surfaces upon helium plasma exposure

Nuclear Materials and Energy 42 (2025) 101883

Figure 1: SEM image in SE mode of three adjacent grains of different orientations showing the nanoholes formed after He plasma exposure at a pressure of 2 Pa, RF power of 400 W, surface temperature of 550°C, ion flux of 2×10^{19} particles $\text{m}^{-2} \text{s}^{-1}$, fluence of 4.5×10^{23} m^{-2} and maximum incident ion energy of 79 eV.

PAUSE PUB:

Ayoub BENMOUMEN, PIIM, **Marseille**, Mesure MET de la taille et du contenu de bulles d'hélium dans des échantillons de tungstène implantés dans le contexte de la fusion nucléaire

POSTERS SESSIONS SCIENCES DE LA MATIÈRE (autour d'un cocktail!!)

Session: Mesure quantitative de propriétés par faisceau d'électrons

MERCREDI 02 JUILLET 17h-19h

CONCLUSION ET PERSPECTIVES

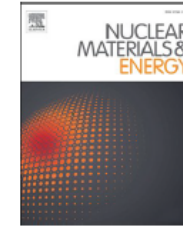
- SEM/EDS essentiel pour la statistique de populations de poussières et dépôts
- La basse tension permet la visualisation de nanoparticules sur une surface
- Travail en synergie avec les expériences TEM/irradiation W au labo
- Continuation de la collaboration pour caractérisation de dépôts et poussières provenant d'autres campagnes WEST



Contents lists available at ScienceDirect

Nuclear Materials and Energy

journal homepage: www.elsevier.com/locate/nme



Dust collection after the high fluence campaign of the WEST tokamak[☆]

C. Arnas^{a,*}, A. Campos^b, M. Diez^c, E. Bernard^c, C. Brun^c, C. Martin^a, F. Gensdarmes^d,
S. Peillon^d, E. Tsitrone^c, the WEST team¹

^a CNRS, Aix-Marseille Université, PIIM, 13397 Marseille, France

^b Aix-Marseille Université, CNRS, Centrale Marseille, FSCM, CP2M, 13397 Marseille, France

^c CEA Cadarache, IRFM, 13108 St-Paul-Lez-Durance, France

^d LPMA, IRSN, 91192 Gif-sur-Yvette, France

ARTICLE INFO

Keywords:

WEST tokamak
Tokamak dust
Tungsten layer flaking
Tungsten nanoparticles

ABSTRACT

For Phase 2 of WEST, the lower divertor was entirely equipped with actively cooled ITER grade plasma-facing units made of chains of tungsten beveled monoblocks. In this configuration, dust particles were collected in 2023, after the first plasma campaign mainly dedicated to repetitive long pulses in the conditions of attached plasmas to the divertor. Due to a high particle fluence and a significant tungsten erosion, large quantities of dust were produced. In addition to those produced during off-normal events and the flaking of deposits which are typical of tokamak wall erosion, dust particles due to the flaking of pure tungsten thin layers deposited on the shadowed areas of beveled monoblocks were found. As specific characteristic, these thin layers may not adhere to the divertor and consequently, may be peeled off and mobilized during plasma operation.

In particular, this diagnostic was used to highlight the presence of nanoparticles with an incident electron beam energy of 5 kV.

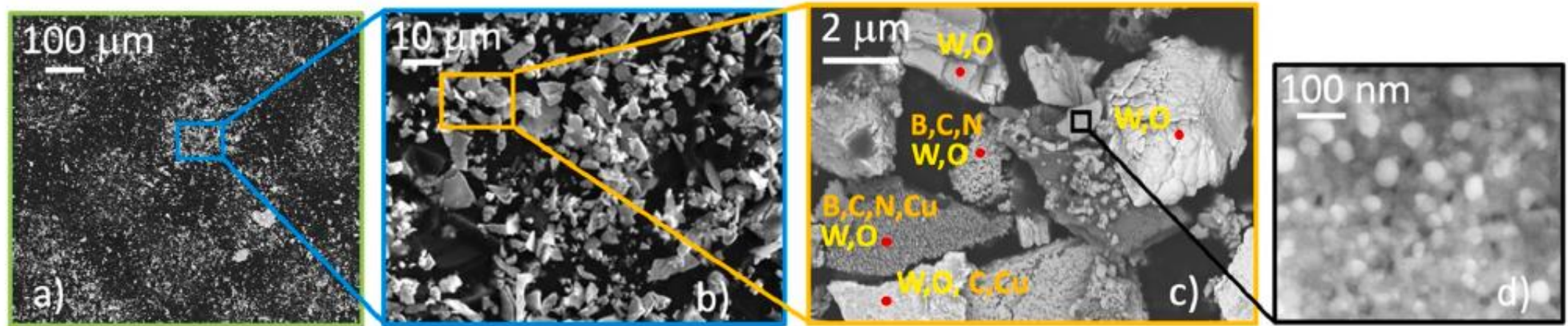
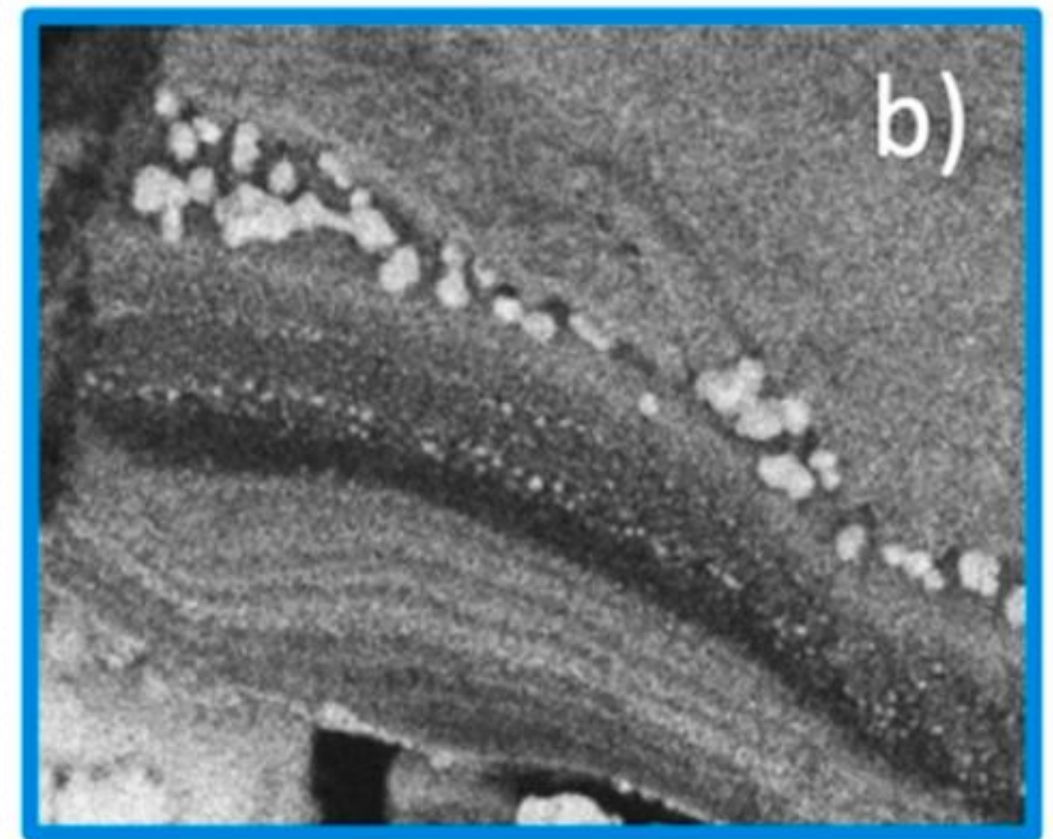
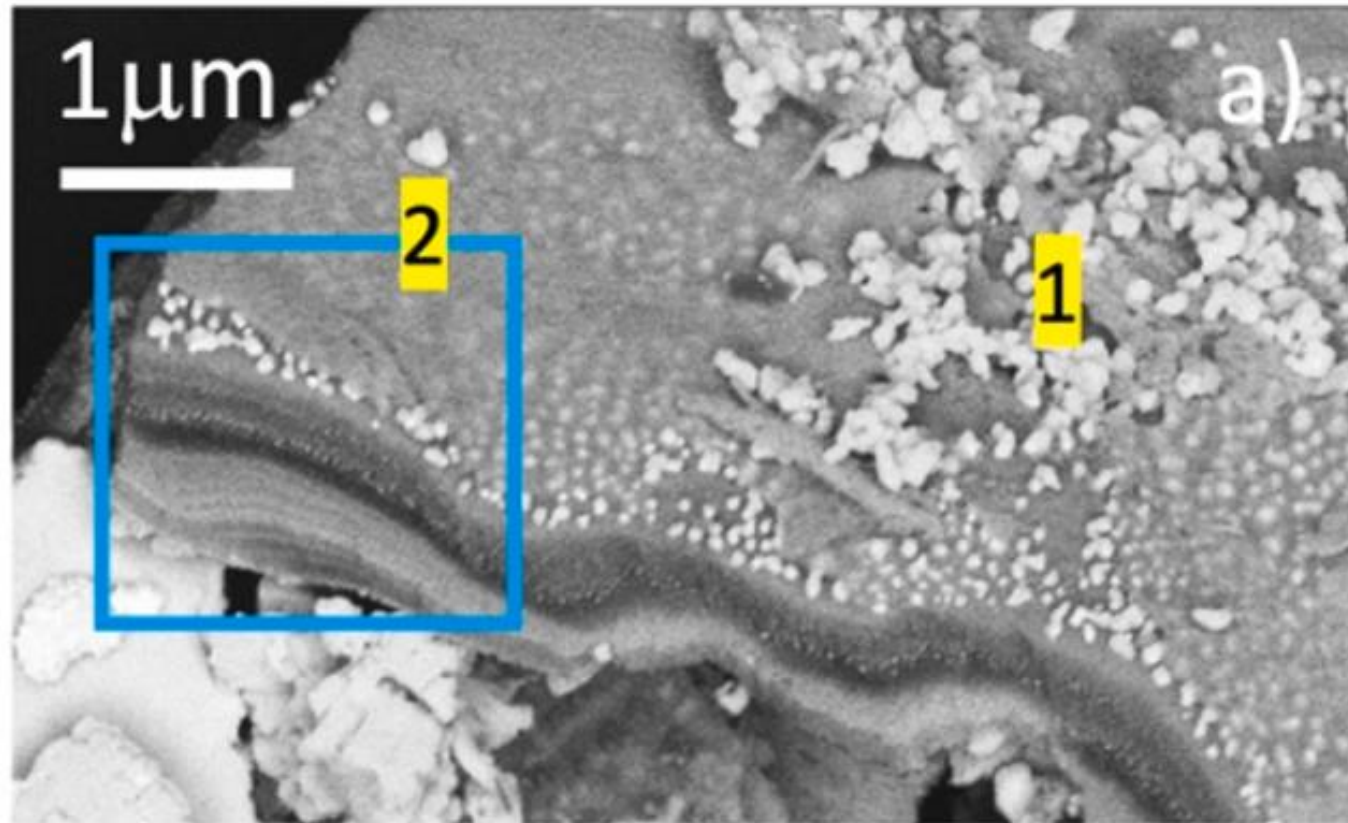
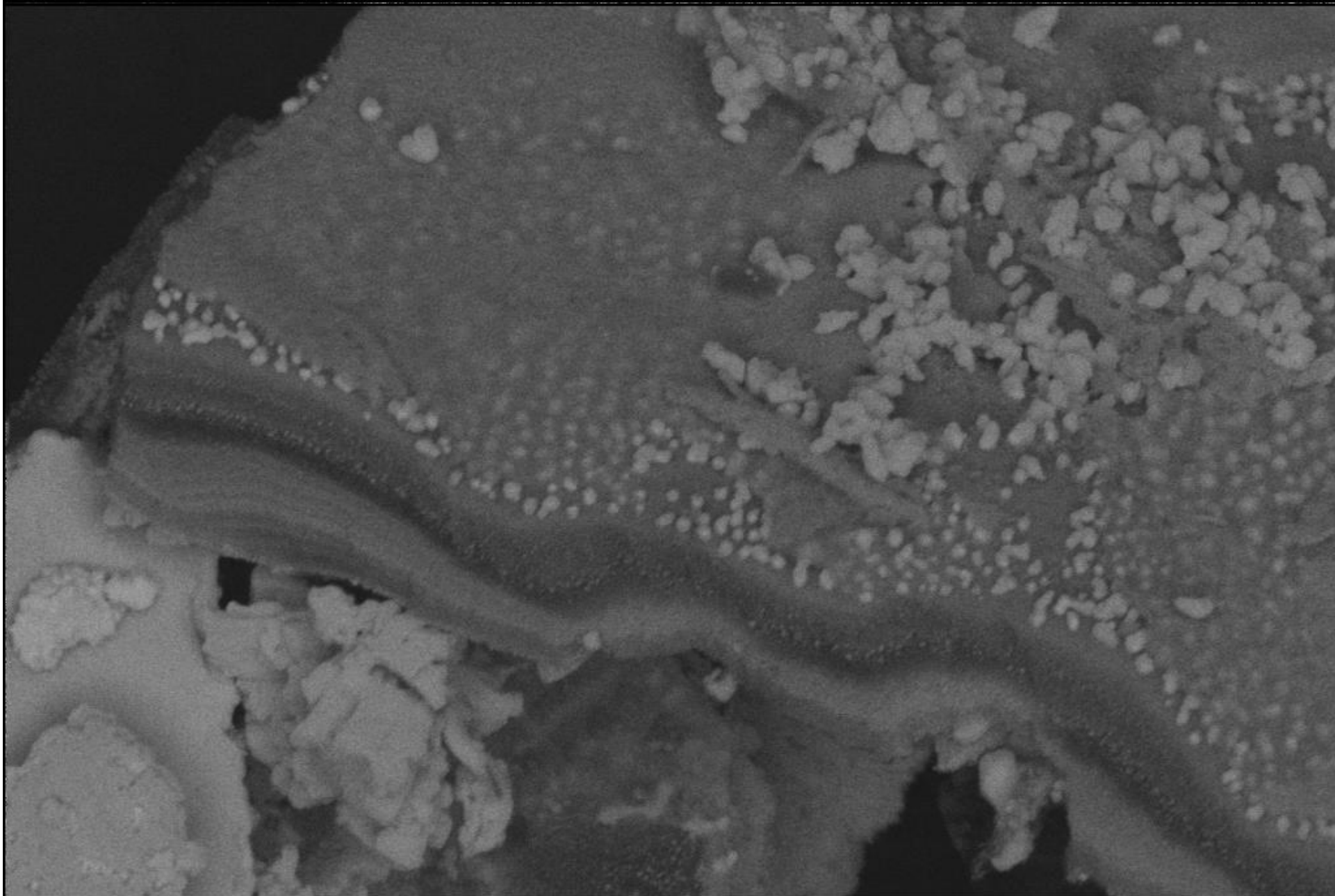


Fig. 3. A) SEM image of a part of the membrane shown [Fig. 1 b](#)). b) and c) details at higher magnifications. c) Compositions of some dust (red dots). d) BSE image showing nanoparticles. (For interpretation of the references to colour in this figure legend, the reader is referred to the web version of this article.)





1 μm

Gemini SEM 500 70-04

EHT = 5.00 kV

WD = 1.3 mm

Signal A = ESB

Mag = 19.59 K X

Pixel Size = 5.699 nm

B = 45.5 % C = 57.4 %

Noise Red. = Drift Comp. Frame Avg.

Scan Speed = 3

Cycle Time = 12.9 Secs

P = 1.33e-06 mbar

Ap. Size = 20.00 μm

27 Oct 2023

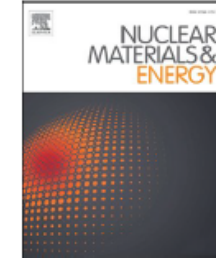
17:06:48



Contents lists available at [ScienceDirect](https://www.sciencedirect.com)

Nuclear Materials and Energy

journal homepage: www.elsevier.com/locate/nme



Post-mortem analysis of the deposit layers on the lower divertor after the 2023 high particle fluence campaign of WEST

C. Martin^{a,*}, M. Diez^b, E. Bernard^b, M. Cabié^c, A. Campos^c, C. Pardanaud^a, G. Giacometti^a, A. Gallo^b, J. Gaspar^d, Y. Corre^b, E. Tsitrone^b, the WEST team¹

^a Aix Marseille Univ, CNRS, PIIM, Marseille, France

^b CEA, IRFM, F-13108 St Paul lez Durance, France

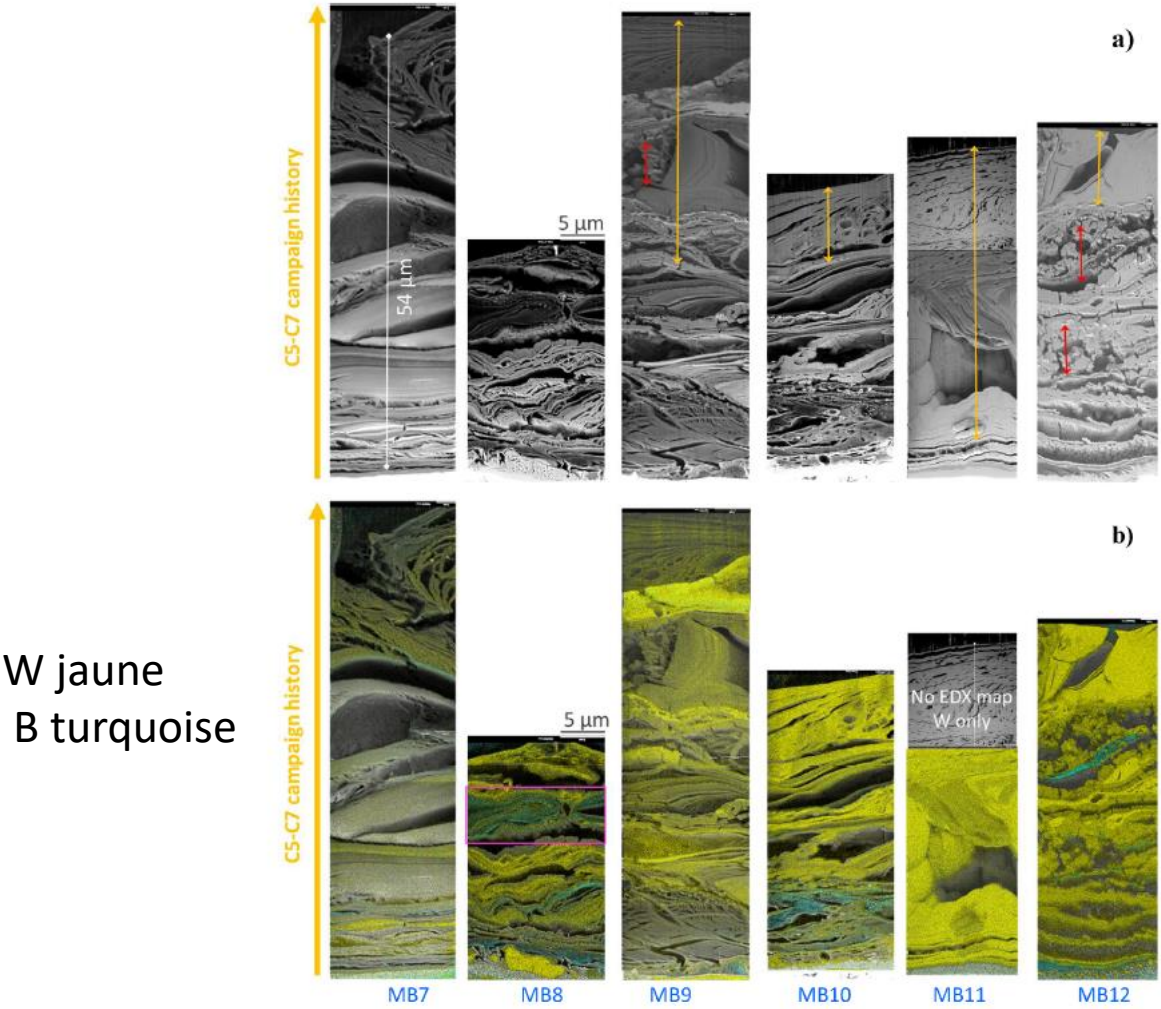
^c Aix Marseille Univ, CNRS, CP2M, Marseille, France

^d Aix Marseille Univ, CNRS, IUSTI, Marseille, France

A B S T R A C T

We analysed deposits collected on the lower divertor of WEST after the first high fluence campaign performed in 2023. Deposits were collected on the high field side (thick deposition area) of 2 ITER-grade plasma facing units (PFUs), located on different toroidal positions. Using focused ion beam cross sectioning, the deposits were found to be very thick (12–55 μm). A significant difference was observed in the toroidal direction with thicker deposits for the PFU located at the maximal heat load in the inner side, showing a deposition pattern due to the toroidal magnetic field modulation. Deposits present a complex layer-by-layer structure with dense layers, some melted parts and porosities within the layers. The deposition is mainly composed of tungsten with oxygen, boron, carbon and traces of nitrogen whose composition vary along the radial direction. We identified W-rich deposits in the high plasma flux area near the inner strike point and deposits rich in O, B, C and N in the low plasma flux area further away from this strike point. W dense layers of about 5 up to 40 μm thick in the thick deposit area near the strike point were attributed to the high fluence campaign. Pure boron layers resulting from wall conditioning and processed by plasma wall interactions were also observed.

Nous avons réalisé une cartographie EDX sur la section transversale avec une énergie incidente de 5 kV et une forte inclinaison de l'échantillon (50–70°), afin d'optimiser la détection des éléments légers tels que B, C, O, N et de minimiser la profondeur sondée pour compenser l'inclinaison



W jaune
B turquoise

Fig. 5. Cross section of deposited layers on the PFU17 of the WEST lower divertor over the C5-C7 campaign history. Thick deposition area displayed from the HFS (left) to the ISP zone (right) along the radial direction from MB7 to MB12 a) SEM images showing the layer by layer structure deposition b) EDX mapping of deposited layers for W (yellow overlay) and B (turquoise overlay). All images are displayed at the same scale, the Y-axis scale is indicated by the white line while the X-axis scale is indicated by the black line. Yellow arrows highlight thick and dense layers of pure tungsten, red arrows highlight the melted area, and the pink frame shows the B + N-rich layer.

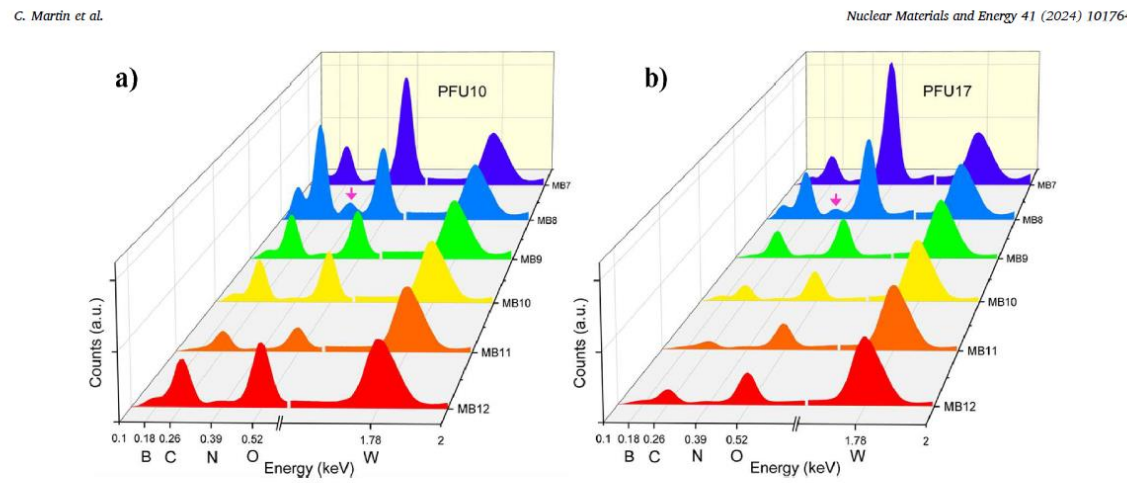


Fig. 6. Sum spectra of EDX mapping area of thick deposit cross-sections normalized by the W peak intensity for MB12 (red) to MB7 (dark blue) a) PFU10 located in the max OSP area b) PFU17 located in the max ISP area.

TEAM



Spectrum Only

Point Analysis

Mapping

Line Scan

Multifield Analysis

Review Data

Report Design

Display Options

Report

Linescan from Map

Rebuild EDS Map



Switch User

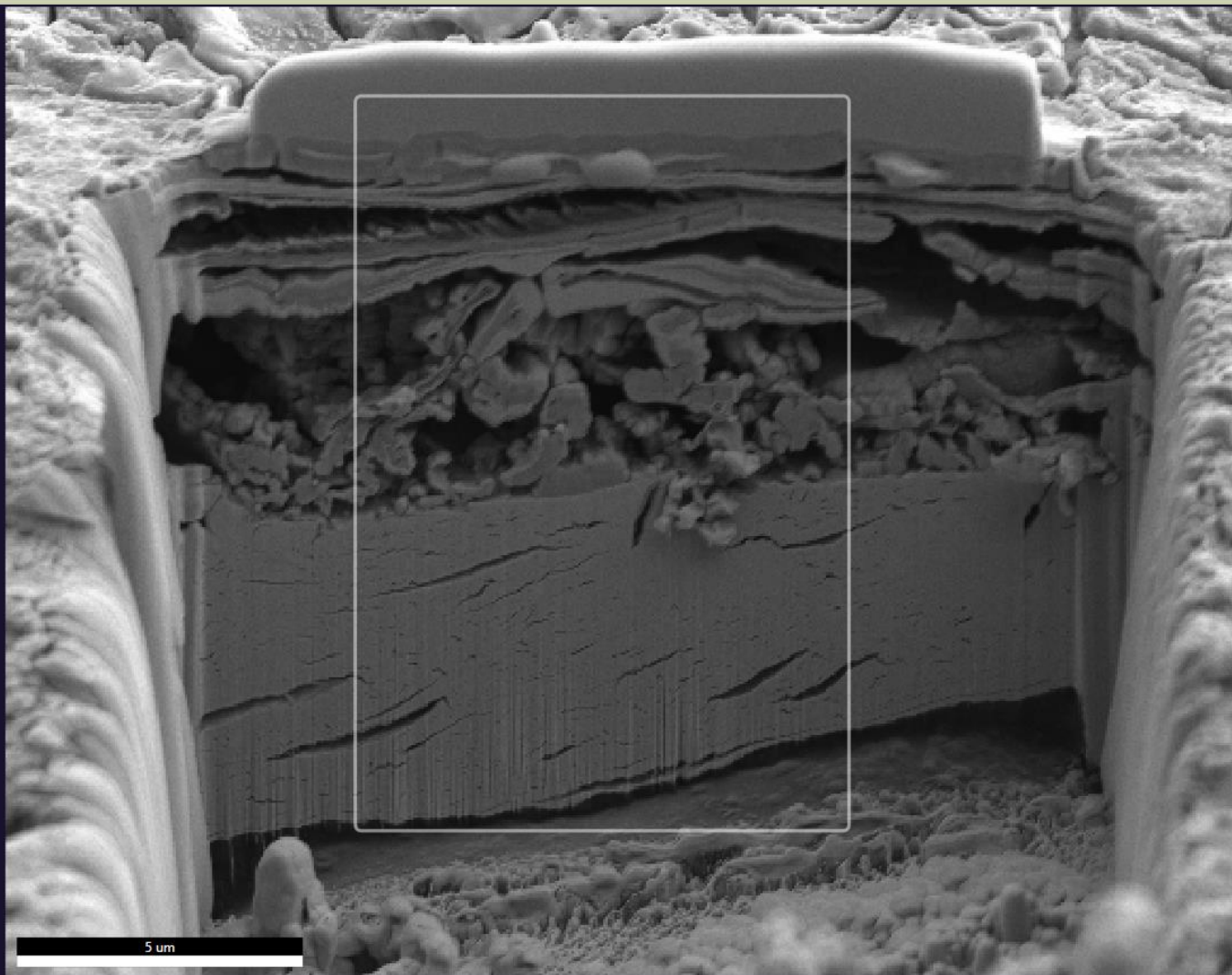
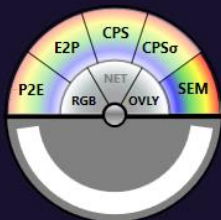
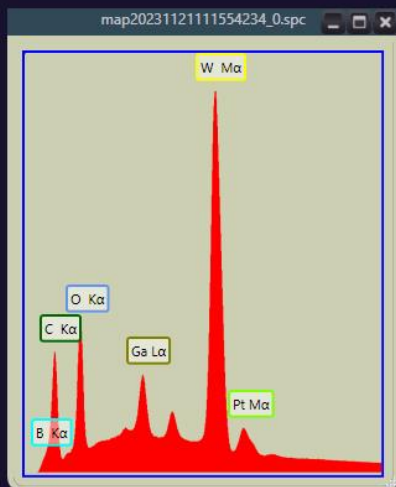
Help

About

EDAX
Smart Insight

administrator

Project Content



Advanced Properties

